The UV/H2O2 Advanced Oxidation Process in UV disinfection units: removal of selected phosphate esters by hydroxyl radical

by

Alexandros Machairas

Diploma in Civil Engineering

National Technical University of Athens, GREECE, July 2003

SUBMITTED TO THE DEPARTMENT OF CIVIL AND ENVIRONMENTAL ENGINEERING IN PARTIAL FULFILLMENT OF THE REQUIREMENTS FOR THE DEGREE OF

MASTER OF ENGINEERING IN CIVIL AND ENVIRONMENTAL ENGINEERING
AT THE
MASSACHUSETTS INSTITUTE OF TECHNOLOGY

JUNE 2004

Signature of Author: _____
Alexandros Machairas
Department of Civil and Environmental Engineering
May 10, 2004

Certified by: _____
Bettina M. Voelker
Associate Professor in Civil and Environmental Engineering
Thesis Supervisor

Accepted by: _____
Heidi Nepf
Chairman, Departmental Committee on Graduate Students

The UV/H2O2 Advanced Oxidation Process in UV disinfection units: removal of selected phosphate esters by hydroxyl radical

by

Alexandros Machairas

Submitted to the Department of Civil and Environmental Engineering

On May 13, 2004 in Partial Fulfillment of the

Requirements for the Degree of Master of Engineering in

Civil and Environmental Engineering

Abstract

In this work, the issue of how to remove phosphate esters from drinking water is examined. From the various treatment processes available, the oxidation of phosphate esters through hydroxyl radical generated by the UV/H2O2 process applied at a UV disinfection unit was selected for evaluation.

The second-order rate constants of the reactions of two phosphate esters, Tri(2-butoxyethyl) phosphate (TBEP) and Tri-2-chloroethyl phosphate (TCEP) , with hydroxyl radical were estimated from our experimental data to be $2 \cdot 10^{10}$ $M^{-1}s^{-1}$ and $2 \cdot 10^{9}$ $M^{-1}s^{-1}$ respectively A comprehensive kinetic model of the oxidation process was derived. Finally computer simulations were used to exhibit the potential of this treatment process and to examine the effects of pH, total carbonate species concentration, initial hydrogen peroxide dose, and light intensity on its efficiency.

The results are not very encouraging when a UV unit designed for disinfection is used. For typical values of pH and total carbonate species (pH=8 and $C_T=5 \cdot 10^{-4}$ M) the 1st order rate coefficients for removal of the phosphate esters are $6.3 \cdot 10^{-4}$ (s^{-1}) for TBEP and $6.3 \cdot 10^{-5}$ (s^{-1}) for TCEP.

If higher light intensity is applied in the reactor (50 times higher), and initial hydrogen peroxide dose of 10^{-3} M and C_T remains $5 \cdot 10^{-4}$ M, the 1st order reaction rate coefficients become $2.9 \cdot 10^{-2}$ (s^{-1}) and $2.9 \cdot 10^{-3}$ (s^{-1}) for TBEP and TCEP respectively.

Thesis Supervisor: Bettina M. Voelker

Title: Associate Professor of Civil and Environmental Engineering

Acknowledgements

The author wishes to express his gratitude to the people who helped him in this current work. The consistent help from my advisor Professor Tina Voelker was invaluable for the completion of this thesis. In addition the assistance of Dr. John Mac Farlane and Dr. Peter Shanahan throughout this work was crucial.

1 INTRODUCTION 5
1.1 EMERGENCE OF ORGANIC WASTEWATER CONTAMINANTS AS A POTENTIAL ENVIRONMENTAL CONCERN 6
1.2 HISTORY OF OCCURRENCE OF OWCS IN NATURAL WATERS 7
1.3 THE SELECTED FAMILY OF CHEMICAL COMPOUNDS – PHOSPHATE ESTERS 8
1.4 REPORTED OCCURRENCES OF THE SELECTED PHOSPHATE ESTERS 9
1.5 DETAILED DESCRIPTION OF SELECTED PHOSPHATE ESTERS 10
1.8 POSSIBLE TREATMENT PROCESSES – UV/H2O2 17
2 EXPERIMENTAL PROCEDURE 19
2.1 MATERIALS 22
2.2 DETAILS OF THE EXPERIMENTAL PROCEDURE 22
2.3 ANALYTICAL PROCEDURE AND DETERMINATION OF REACTION RATE CONSTANTS 25
2.4 ANALYSIS AND STATISTICAL MANIPULATION OF THE GCMS RESULTS 28
2.5 A PROBABILISTIC APPROACH FOR THE RATE CONSTANTS 39
2.6 EXPERIMENTALLY DERIVED RATE CONSTANTS 42
3 A THEORETICAL APPROACH FOR THE RATE CONSTANTS OF THE PHOSPHATE ESTERS WITH HYDROXYL RADICAL 43
3.1 DETERMINING UPPER LIMITS FOR THE REACTION RATE CONSTANTS OF THE PHOSPHATE ESTERS WITH HYDROXYL RADICAL 43
3.2 EFFECTS OF STRUCTURE OF THE PHOSPHATE ESTERS ON THEIR REACTION RATE CONSTANTS 45
3.3 DISCUSSION ON REACTION RATE CONSTANTS AND CLOSURE 48
4 THE H_2O_2/UV OXIDATION PROCESS 49
4.1 CONCEPTUAL MODEL OF THE ULTRA VIOLET DISINFECTION UNIT 53
4.2 CHARACTERISTICS OF OUR IDEAL UV REACTOR 55
4.3 IMPLEMENTING THE MODEL OF H_2O_2/UV ADVANCED OXIDATION PROCESS 59
4.4 ISSUES ABOUT IMPLEMENTING THE MODEL IN MATLAB 68
5 RESULTS OF THE MODEL 69
5.1 SOLUTION RECIPE AND EFFICIENCY OF THE PROCESS 73
5.2 EFFECTS OF PH 73
5.3 EFFECTS OF C_T 76
5.4 EFFECTS OF INITIAL HYDROGEN PEROXIDE DOSE 77
5.5 EFFECTS OF LAMP POWER 80
5.6 STEADY STATE CONSIDERATIONS AND QUICK AND DIRTY CALCULATIONS 81
5.7 ATLANTA WATER WORKS 89
6 CONCLUSIONS 93
7 BIBLIOGRAPHY 96

1 Introduction

Organic Wastewater Contaminants (OWCs) are an emerging concern in environmental sciences. Their presence has been reported in natural waters and even in treated drinking water. The present work aims at evaluating the potential removal of these contaminants through altering already existing treatment processes at Drinking Water Treatment Plants (DWTPs).

From the vast numbers of reported OWCs the present work focuses on three phosphate esters, tributyl phosphate (TBP), tri(2-chloroethyl) phosphate (TCEP) and tri(2-butoxyethyl) phosphate (TBEP). As a removal process, ultraviolet disinfection with addition of hydrogen peroxide is considered. This process generates hydroxyl radicals ($OH\bullet$) which are powerful oxidants.

The reaction rate constants of the phosphate esters with hydroxyl radicals are derived through experiments and a chemical kinetic model is developed for the advanced oxidation treatment process. Finally computer simulations of the model are carried out to investigate the removal potential and the various parameters that affect it.

1.1 Emergence of Organic Wastewater Contaminants as a Potential Environmental Concern

One of the main current concerns in environmental sciences is the increasing occurrence of organic wastewater contaminants in the natural water environment. The problem was first identified in the late seventies, and throughout the last twenty-five years, there have been an increased number of reports of presence of these chemical compounds in natural water systems.

The concentrations measured range from on the order of a few nanograms per liter in surface waters to a few micrograms per liter in wastewater effluents. For most substances, such concentrations do not pose an immediate threat to the environment and human health but are alarming because the effects and fate of these anthropogenic chemicals in the environment are not clearly understood. Currently most research is targeted at pharmaceuticals, because they are highly active compounds that are engineered to be persistent and the chronic effects of low-level exposure are not understood. Besides pharmaceuticals, other major groups of anthropogenic organic chemical compounds have been detected in the water environment in comparable concentrations.

One of these groups is the phosphate esters that are primarily used as flame-retardants and plasticizers. Even though their nature and use suggest that they would be mainly found in industrial effluents, they have been reported in a wide range of water systems and even in drinking water distribution networks.

1.2 History of occurrence of OWCs in natural waters

Since the early eighties, studies reporting the occurrence of anthropogenic organic chemicals in the water environment were made in Europe. They mainly focused on pesticides in river and lake systems. Around the same time, studies in Japan revealed the presence of industrial organic chemicals in surface waters and in municipal and industrial wastewaters. In Canada studies as early as 1979 identified anthropogenic organic chemicals in drinking water.

In response to the emerging environmental concerns regarding organic wastewater contaminants (OWCs), the U.S Geological Survey conducted the first nationwide reconnaissance of the occurrence of these chemical compounds in U.S. streams and rivers (Kolpin et al., 2002) in 1999-2000. The results were surprising since OWCs were found in 80% of the streams sampled.

Following the findings of the USGS reconnaissance, the Centers for Disease Control and the USGS initiated a study to determine the occurrence and fate of commonly used pharmaceuticals and organic chemical compounds in surface and drinking waters of a large metropolitan city. The selected study site was a portion of the Chattahoochee River and one of its tributary streams, Big Creek, located north of Atlanta, Georgia.

This is the most extensive study conducted in the United States and the only one that provides information on the fate of the selected chemicals in a river system and in the treatment processes. Again the findings are shocking since a substantial number of OWCs and pharmaceuticals were detected in finished drinking water at comparable concentrations to those found in the river system before drinking water treatment plant uptakes.

1.3 The Selected Family of Chemical Compounds – Phosphate Esters

This group is comprised of three phosphate esters: tributyl phosphate (TBP, CAS #126-73-8), tri(2-chloroethyl) phosphate (TCEP, CAS # 115-96-8), and tri(2-butoxyethyl) phosphate (TBEP, CAS # 78-51-3). These phosphate esters have been chosen based on the following reasons:

- The CDC-USGS study detected these compounds in most of the samples.
- Many other studies report the presence of these compounds in surface water and drinking water.
- All three phosphate esters exhibit some similar chemical characteristics, where other chemicals in the CDC-USGS study having a high percentage of detection did not exhibit similar properties.
- They are widely used as flame retardants, plasticizers, and other various products.
- They exhibit significant persistence in the environment.

1.4 Reported Occurrences of the Selected Phosphate Esters

Drinking Water

Reports of occurrence of the selected organophosphates exist from as early as 1979 in a national survey of Canadian drinking water. The concentrations reported were 0.2 to 62 ng/L for TBP, 1.1 to 560 ng/L for TBEP and 0.3 to 13.8 ng/L for TCEP (HSDB Database).

All three of the selected organophosphates have been identified as present in the drinking water in the CDC survey.

Surface Waters

TBP has been reported in surface waters in the U.S. (CDC), Japan, Spain, Italy, Germany, Switzerland, and the U.K. (HSDB database). Reported concentrations are below 1 μg/L.

TBEP has been reported in surface waters in the U.S. (Kolpin et al., 2002), Japan, Sri-Lanka, and Germany (HSDB database). Reported concentrations are up to a few micrograms per liter.

TCEP has been reported in surface waters in the U.S. (Kolpin et al., 2002), Japan, and Italy at concentrations below 0.5 μg/L (HSDB database).

Treatment Plant Effluents

In a comprehensive survey of wastewater from 4000 industrial and publicly owned treatment works (POTWs) sponsored by the Effluent Guidelines Division of the U.S. EPA, TBP was identified in various types of industrial discharge. The maximum industrial effluent concentrations were 13.5 mg/l in the organics and plastics industry and 10.0 mg/l in the paint and ink industry (HSDB database).

Groundwater

TBP and TCEP have been reported present in the groundwater at concentrations up to 200 ng/L in the U.S, Spain, and the Netherlands (HSDB database).

1.5 Detailed Description of Selected Phosphate Esters

The three compounds being studied are tributyl phosphate, tri(2-butoxyethyl) phosphate and tri(2-chloroethyl) phosphate. They are members of the phosphate ester family of chemicals which are the predominant phosphate-containing flame retardants in use. Phosphate ester flame retardants represent twenty percent of the worldwide production of flame retardants (Environmental Health Criteria-192, 1997).

In general, the phosphate ester flame retardants work by breaking down into phosphoric acid and other components upon heating. The phosphoric acid forms a char on the surface of the material being burned, thus shielding the substance from being burned by the heat and stopping the release of volatiles being combusted. In addition, free radicals are formed and released into the vapor phase. The free radicals compete for the materials being oxidized in the combustion reaction, thereby reducing the intensity of the flame (Environmental Health Criteria-192, 1997).

Tributyl Phosphate

Tributyl phosphate (TBP) is an anthropogenic chemical that has flame retardant abilities and is used in plastics, floor finishes, hydraulic fluids and ore extraction processes

Physical Properties

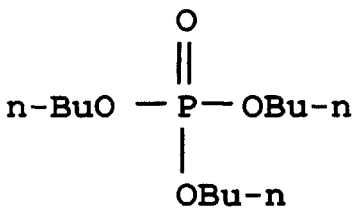

Figure 1-1 TBP

The chemical formula for TBP is $C_{12}H_{27}O_4P$, and its structure is shown above. At room temperatures, TBP is a colorless and odorless liquid which is non-explosive and non-flammable. (Environmental Health Criteria–112, 1991)

Some of the relevant physical properties of TBP are:

- A molecular weight of 266 g
- a maximum solubility in water of 280 mg/L
- a vapor pressure of 0.00113 mmHg
- a Henry's Law constant of 1.41 x 10^6 atm-m^3/mole at 20 °C

(SRC Physprop Database, December 1, 2003)

Manufacture and Uses

TBP is manufactured through the reaction of butyl alcohol and phosphorous oxychloride (Toxinet database). It is manufactured under the brand names Phosflex 4,

Skydrol LD-4, Celluphos 4, and Disphamol 1 TBP (Environmental Health Criteria-112, 1991).

There are several manufacturers, some of which are: Pfletz & Bauer Inc., Akzo Nobel, Acros Organics USA, Chem Service, Inc., ICN Biomedicals, and Wako Chemicals USA (Environmental Health Criteria–112, 1991).

The major use (forty to sixty percent) of TBP is in fire resistant hydraulic fluid for aircraft. (Environmental Health Criteria–112, 1991)

The second most prevalent use of TBP is as a plasticizer for plastics and vinyl resins. It is a preferred plasticizer due to its dual capability as a plasticizer and flame retardant in plastics.

An interesting, emerging use of TBP is in the recovery of uranium ores from reactor products. This use of TBP has become increasingly significant in recent years (Thomas et al., 1998; Environmental Health Criteria–112, 1991).

1.6 Tri(2-butoxyethyl) Phosphate

Tri(2-butoxyethyl) phosphate (TBEP) is an anthropogenic chemical used in floor polishes and as a plasticizer in rubbers and plastics. TBEP acts also as a flame retardant.

Physical Properties

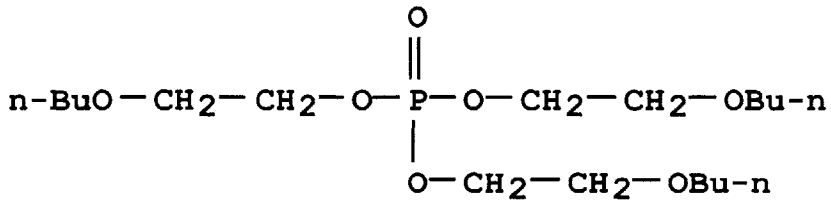

Figure 1-2 TBEP

The chemical formula for TBEP is C18H39O7P, and its structure is shown above. At room temperatures it is a light-colored, viscous fluid with an odor of butyl. It is a non-flammable substance with a high boiling point (413.9 °C). (Environmental Health Criteria–218, 2000)

Some of the relevant physical properties of TBEP are:

- a molecular weight of 398.5 g
- a maximum solubility in water of 1100 mg/L
- a vapor pressure of 2.5E-8 mmHg
- a Henry's Law constant of 1.2 x 10^{-11} atm-m^3/mole at 20 °C

(SRC Physprop Database, December 1, 2003)

Manufacture and Uses

TBEP is manufactured through the reaction of butoxyethanol and phosphorous oxychloride and stripping hydrochloric acid in excess of butoxyethanol (Environmental Health Criteria–218, 2000).

It is manufactured under the brand names Kronitex KP-140, KP-140, Phosflex T-BEP, Phosflex 176C, and Amgard TBEP (INCHEM, Environmental Health Criteria–218, 2000).

Manufacturers in the United States include City Chemical LLC, Pfletz & Bauer Inc., Akzo Nobel, Acros Organics USA, Chem Service, Inc., Scientific Polymer Products Inc., Ashland Distribution Company, ICN Biomedicals and Wako Chemicals USA (Chem Sources).

The most likely pathway through which TBEP gets into the waste water system is through its use in floor polishes. TBEP adds elasticity and gloss to floor polishes. The increased elasticity increases the leveling and spreading properties of the polish. It is a component of several household floor polishes, including such familiar names as Mop & Glo and Brilliance, in concentrations as high as eight percent. (Household Products Database) Disposal of wastewater after floor polishing is an obvious pathway to municipal wastewater systems.

1.7 Tri-2-chloroethyl phosphate

Tri-2-chloroethyl phosphate (TCEP) is an anthropogenic chemical used as a fire retardant and plasticizer in liquid unsaturated polyester resins and PVC and as a fire resistant back coating for textiles.

Physical Properties

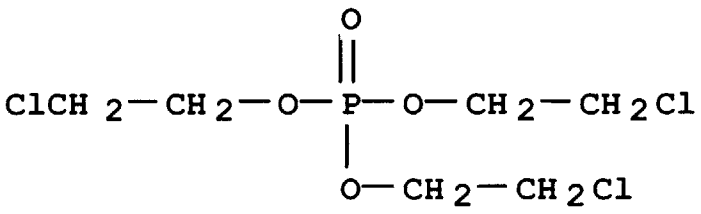

Figure 1-3 TCEP

The chemical formula for TCEP is C6H12Cl3O4P and its structure is shown above. At room temperatures it is a clear, colorless liquid with a slight odor. It decomposes at temperatures above 220 °C (Environmental Health Criteria–209, 1998).

Some of the relevant physical properties of TCEP are:

- a maximum solubility in water of 8000 mg/L
- a vapor pressure of 0.0612 mmHg
- a Henry's Law constant of 3.29 x 10^{-6} atm-m^3/mole at 20 °C

(SRC Physprop Database, December 1, 2003)

Manufacture and Uses

TCEP is manufactured through the reaction of phosphorous oxychloride with ethylene oxide followed by subsequent purification (Environmental Health Criteria–209, 1998).

It is manufactured under the brand names Celanese Celluflex CEF, Celluflex CEF, Disflamoll TCA, Fyrol CEF, Fyrol CF, Genomoll P, Niax 3CF, Niax Flame retardant 3 (nospaa)CF, Hosta flam UP 810, Amgard TCEP, Tolgard TCEP, Antiblaze TCEP, Levagard EP, and Nuogard TCEP (INCHEM, Environmental Health Criteria–209, 1998).

Manufacturers in the United States include City Chemical LLC, Pflatz & Bauer, Inc., Akzo Nobel Functional Chemical, and Acros Organics USA.

TCEP has several uses that provide ready pathways into the municipal wastewater stream. TCEP is used as fire retardant in liquid unsaturated polyester resins (Environmental Health Criteria–209, 1998). The normal concentration is 2-5 % in these resins. (Jiangdu Dajian Chemical Factory web site) The resins are used in the casting of

bathtubs, spas, and pipes. It is possible that leaching from these surfaces could provide a pathway into the environment.

An even more likely pathway into the environment is the use of TCEP as a back-coating for textiles used in furniture and protective clothing. Maintenance and cleaning of these products and subsequent disposal of the wastewater used in the process could provide a pathway to the wastewater treatment plant (WWTP) (Environmental Health Criteria–209, 1998).

1.8 Possible treatment processes – UV/H2O2

Currently there are no immediate concerns regarding the removal of organic wastewater contaminants during drinking water treatment. There are more urgent needs to be addressed like pathogenic micro-organisms such as cryptosporidium and toxic metals such as arsenic. This of course does not mean that OWCs can be neglected. Their chronic effects on human health have not been assessed and fears exist that they might prove harmful even at these very low concentrations. OWCs are anthropogenic compounds which do not occur naturally at the environment and certainly their presence in drinking water is not desirable.

Advanced Oxidation Processes (AOPs) were identified as the most promising processes for the removal of the phosphate esters at DWTPs. Advanced oxidation processes are based on generating reactive radicals, mainly hydroxyl radical, which oxidize the target organic pollutants. Alternative treatment processes are granular activate carbon (GAC) filtration or membrane micro filtration. These processes have a significant cost and especially GAC efficiency is limited to only hydrophobic compounds.

Currently the AOPs proposed in the literature are UV/H2O2, O3/UV, O3/UV/H2O2 and UV/TiO2 systems. All of the above systems generate hydroxyl radicals as the main oxidant. From these systems, UV/H2O2 was selected for the current work.

The hydrogen peroxide ultraviolet light system was selected because its reaction mechanism is well researched and understood. In addition the UV disinfection reactors are designed to mimic plug flow reactors enabling an accurate and simple model of the progress of the chemical process. Finally ultraviolet disinfection is expected to become more popular in the near future since it has been proven to inactivate cryptosporidium, which is required by the Long Term 2 Enhanced Surface Water Treatment Rule (LT2ESWTR) currently in development by EPA.

Implementing the UV/H2O2 system in a UV disinfection unit would just require a rapid mixing tank prior to the UV reactor for the mixing of hydrogen peroxide. Therefore no substantial capital costs or engineering problems are involved with implementing such a system. In addition hydrogen peroxide is a relatively cheap chemical; the average price per pound in 2000 was 4 cents/lb (http://www.manufacturing.net/pur/article/CA154359).

The aim of the current work is to assess the efficiency of the UV/H2O2 advanced oxidation process, when applied in UV disinfection units, to remove the selected phosphate esters. The main oxidizing agent in this process is hydroxyl radical. An accurate knowledge of the reaction rate constants of the phosphate esters with hydroxyl radical is essential to the model that will be developed. Since the second-order rate constants were not known (except for TBP) the first step for this work was to derive the reaction rate constants through experiments.

Having derived the reaction rate constants our next step was to model conceptually the advanced oxidation process. The reaction mechanism had to be considered and the UV unit was modeled as a reactor tank. In addition the specifications of the UV reactor were defined, which proved to be very difficult. Finally issues about the implementation of the model were addressed.

At this stage the model was ready to be used and the efficiency of the process was evaluated. The chemistry of natural waters is complicated and various parameters affect the removal potential. Each of these parameters was considered and the effects the process were investigated.

2 Experimental procedure

When designing experiments to estimate the rate constant of a chemical compound with hydroxyl radical, two major decisions must be made: how to generate hydroxyl radical, and how to conduct the experiments so that the rate constants can be derived from them. For a compact review of mechanisms for generating hydroxyl radical and methods for deriving reaction rates the reader is referred to Buxton et al (1988).

In the present work, hydroxyl radicals were generated using the Fenton reaction and the rate constants were obtained through a competition method.

The Fenton reaction was chosen because of its simplicity. The reaction mechanism consists of the oxidation of ferrous iron to ferric iron by hydrogen peroxide with products hydroxide ions and hydroxyl radicals.

$$Fe^{+2} + H_2O_2 \rightarrow OH\bullet + Fe^{+3} + OH^- \qquad (2.1)$$

This reaction was the one primarily used for the generation of hydroxyl radicals until radiolysis and sonolysis of water were developed. Therefore extensive literature exists (though somewhat old) on how to conduct the experiments, which helped the design process of the experiments.

The competition method is a very widely used method to derive reaction rate constants when direct measurement of the reaction progress is difficult or impossible. The method is based on knowing the reaction rate constant of a chemical compound with hydroxyl radical that will act as the reference compound. If the chemical compound whose reaction rate constant with hydroxyl radical we wish to measure does not react with the reference compound, and neither compounds react with any other species present during the experiment, these two compounds will be competing for the hydroxyl radicals present in the solution. Therefore the reactions through which the reference compound R and the other compound A are lost in the experimental solution are:

$$\begin{aligned} R + OH\bullet &\rightarrow^{k_R} \text{Products R} \\ A + OH\bullet &\rightarrow^{k_A} \text{Products A} \end{aligned} \qquad (2.2)$$

For each of the two chemical compounds, we can write the differential equation governing its concentration.

$$\begin{aligned} \frac{d[R]}{dt} &= -k_R \cdot [R] \cdot [OH\bullet] \\ \frac{d[A]}{dt} &= -k_A \cdot [A] \cdot [OH\bullet] \end{aligned} \qquad (2.3)$$

Where [R], [A] and [OH•] are the molar concentrations (moles/liter) of compound R, compound A and hydroxyl radical respectively. Using simple algebraic manipulations a relationship between the two reaction rate constants can be established.

$$\frac{dA}{[A]} \cdot \frac{1}{[OH\bullet] \cdot k_A} = \frac{dR}{[R]} \cdot \frac{1}{[OH\bullet] \cdot k_R} = -dt \qquad (2.4)$$

crossing out hydroxyl radical and integrating

$$\frac{1}{k_A} \cdot \int \frac{dA}{[A]} = \frac{1}{k_R} \cdot \int \frac{dR}{[R]} \qquad (2.5)$$

$$\frac{1}{k_A} \cdot \ln[\frac{[A]_t}{[A]_{t-1}}] = \frac{1}{k_R} \cdot \ln[\frac{[R]_t}{[R]_{t-1}}] \qquad (2.6)$$

$$k_A = k_R \cdot \left(\ln[\frac{[A]_{t-1}}{[A]_t}] / \ln[\frac{[R]_{t-1}}{[R]_t}] \right) \qquad (2.7)$$

Therefore, the ratio of the rate constants is a function of how much of each compound was consumed during the reaction.

The competition method can be applied to any given time advancement of the reaction. In this work, we consider the initial conditions (prior to generating hydroxyl

radicals) and the final conditions, when the reaction has come to completion. This method has the significant advantage that it does not require monitoring the progress of the reaction and taking samples while the reaction is proceeding. To obtain the rate constant k_A, the only measurements needed are the initial and the final concentrations of the two chemical compounds. The equation for deriving the rate constant is then:

$$k_A = k_R \cdot \left(\ln[\frac{[A]_0}{[A]_\infty}] / \ln[\frac{[R]_0}{[R]_\infty}] \right) \quad (2.8)$$

This method can also be used with more than two chemical compounds present simultaneously in the experimental solution.

The only potential problems with this competition method are that the reacting chemical compounds must be present at detectable limits after the reaction has come to completion and that significant consumption of the reacting compounds must take place so that it is easily measured. When using the Fenton reaction to generate hydroxyl radicals one way to ensure that the reacting chemical compounds will be present at detectable concentrations after the reaction has come to completion is by adding hydrogen peroxide at a lower concentration than the reacting chemicals. However, the concentration chosen must also be high enough to cause significant consumption of the compounds.

In this work the goal of our experiments is to measure the reaction rate constants of two of the three phosphate esters of interest, (TCEP and TBEP). Because the reaction rate constant of TBP with hydroxyl radical is known (Buxton et al 1988), it was chosen as the reference compound.

2.1 Materials

The chemical compounds used in the experiments were all reagent grade. For the solution distilled water was used. Tributyl Phosphate was from Fluka Chemie GmbH and Tris (2 butoxyethyl) Phosphate and Tris (2-chloroethyl) Phosphate were from Sigma-Aldrich. Ferrous Ammonium Sulfate $Fe(NH_4)_2(SO_4)\cdot 6H_2O$ came from Mallincrodt Chemical Works and Hydrogen Peroxide from EM Science.

2.2 Details of the experimental procedure

As was mentioned before, the experimental procedure chosen involves generation of hydroxyl radicals using Fenton reaction and estimation of the reaction rate constants using the competition method. The design of the experiments followed the one used by Haag and Yao (1992).

The reaction solution was designed to have concentrations of 500 μM Fe^{+2}, 100 μM TBP, TBEP and TCEP and varying concentrations of H_2O_2 (60-150 μM). The concentration of H_2O_2 was varied between experiments to obtain different levels of oxidation for the phosphate esters. This approach was used to detect possible effects of the initial concentration of hydrogen peroxide on the reaction rate constants.

The experiments were performed in the following way:

A stock solution of 1 L of the ferrous iron and the phosphate esters was prepared and the pH of the solution was set at pH = 3 by adding 1ml of nitric acid [1M] to prevent iron from oxidizing.

The exact concentrations of the phosphate esters were 91.7 μM TBP, 118.0 μM TCEP and 118.7 μM TBEP. These concentrations were chosen to correspond to exact volumes of available micropipettes (50 μL and 25 μL).

From the stock solution, 100 ml was transferred to reaction vessels. In the reaction vessels, hydrogen peroxide was then added so that the reaction would commence.

An estimate of the required time for the completion of the reaction can be made by solving the system of differential equations governing the reaction.

$$\begin{aligned}
\frac{d[Fe(II)]}{dt} &= -k_1 \cdot [Fe(II)] \cdot [H_2O_2] \\
\frac{d[H_2O_2]}{dt} &= -k_1 \cdot [Fe(II)] \cdot [H_2O_2] - k_2 \cdot [OH\bullet] \cdot [H_2O_2] \\
\frac{d[OH\bullet]}{dt} &= k_1 \cdot [Fe(II)] \cdot [H_2O_2] - k_2 \cdot [OH\bullet] \cdot [H_2O_2] - k_{TBP} \cdot [OH\bullet] \cdot [TBP] \\
\frac{d[TBP]}{dt} &= -k_{TBP} \cdot [OH\bullet] \cdot [TBP]
\end{aligned} \qquad (2.9)$$

where k1 is 76 $M^{-1}s^{-1}$ at pH 3, k2 is $2.7*10^7$ $M^{-1}s^{-1}$ and kTBP is 10^{10} $M^{-1}s^{-1}$

In this simplified model the scavenging of hydroxyl radicals by the phosphate esters is lump summed as an effect of only TBP. Solving the system of differential equations we can follow the progress of the reaction. For the reaction sample with the highest dose of hydrogen peroxide (150 μM) the results are presented in figure 1-1.

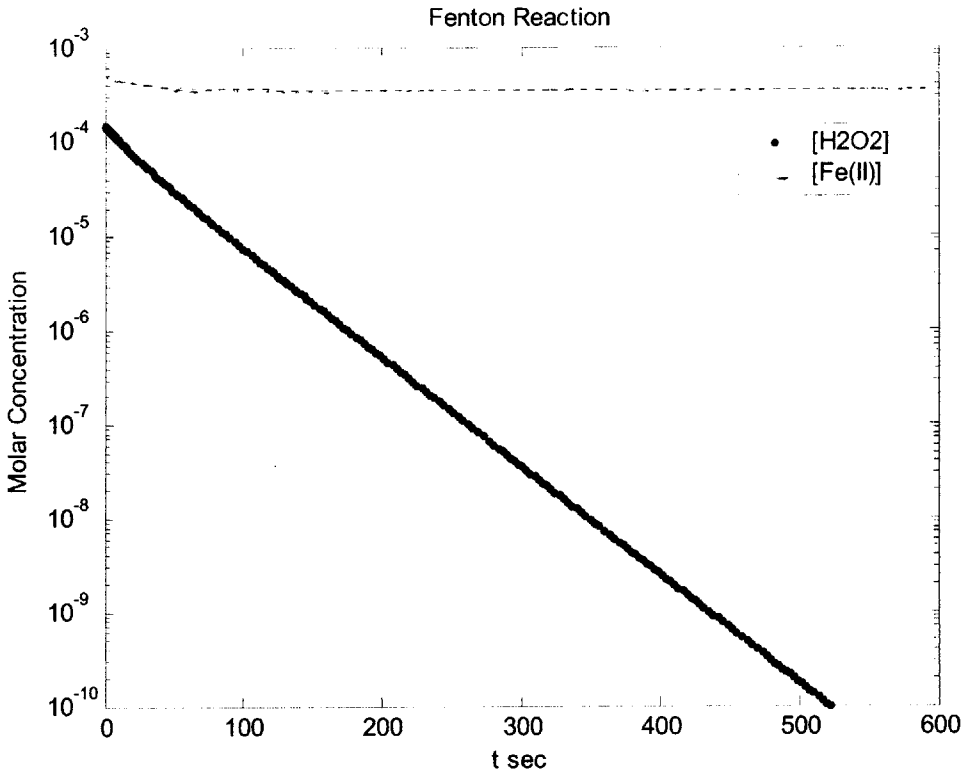

Figure 2-1 Progress of the Fenton reaction

From figure 1-1 it is evident that the reaction has come to completion after 10 minutes have passed from the addition of hydrogen peroxide (the concentration of H_2O_2 is below 10^{-10} M).

In the competition method monitoring the progress of the reaction is not needed, the concentrations of the reacting compounds only need to be measured at any point after completion of the reaction. Due to logistical reasons the samples were left in the reaction vessels for 24 hours. The pH of the reaction sample was measured to confirm that it had remained constant through the reaction. In all of the experiments the pH had not changed.

After the specified time, 50 ml from the reaction sample were transferred to a separation funnel and triple extraction into methylene chloride was performed. After extraction to methylene chloride the samples were stored at a constant temperature

of 4 °C. The extracts were treated with sodium sulfate to dehydrate them, and the volume of the final extract was determined through weighing the vials that contained them empty and full.

Two series of experiments were performed, the first one as a training exercise and in order to identify possible experimental errors. From the first series of experiments, several errors were identified that were associated with the experimental procedure. No data will be reported for this series of experiments.

The second series of experiments consisted of the following samples (with regard to the added concentration of hydrogen peroxide):

Table 2.1 Experimental Samples

Experiment	H2O2 μM
2.1	60
2.2	90
2.3	120
2.4	150
2.5	0

All of the results to follow refer to this series of experiments.

2.3 Analytical procedure and determination of reaction rate constants

The competition method is based on having a reactant with a known reaction rate constant with hydroxyl radical. The rate constant of TBP with hydroxyl radical is k = 1.0×10^{10} $M^{-1}s^{-1}$ (Buxton et al. 1988) and TBP was used as the reference compound.

The initial and the final concentration of the various reactants in the mixture are measured and the reaction rate constants are obtained from the following expression (here written for TCEP).

$$K_{\text{TCEP,OH}\cdot} = \frac{\ln([\text{TCEP}]_0 / [\text{TCEP}]_\infty)}{\ln([TBP]_0 / [TBP]_\infty)} \cdot K_{\text{TCEP,OH}\cdot} \qquad (2.10)$$

The samples were analyzed in an HP 6890 Gas Chromatograph equipped with an HP 6890 auto sampler injector, with a JEOL GC-Mate Mass Spectrometer . The column used was a ZB-5 Zebron Capillary GC Column with dimensions 30m * 0.25 mm * 0.50 μm which was 5% phenyl and 95% dimethyl-poly siloxane.

The elution sequence used is presented in the next table:

Table 2.2 Elution sequence

T (°Celsius)	Time (min)	Rate of change (°Celsius/min)
70	1	20
150	0	10
300	5	0

The carrier gas was helium, with a flow rate of 2 ml/min. The injection procedure was splitless for 1 minute under constant flow, with an inlet temperature of 300 °C.

The method used for the MS analysis was selected ion monitoring. The characteristic mass:charge ratios for the phosphate esters were obtained from the standard reference library. The mass:charge ratios used were 99.3, 63.2 and 57.3 for TBP, TCEP and TBEP respectively

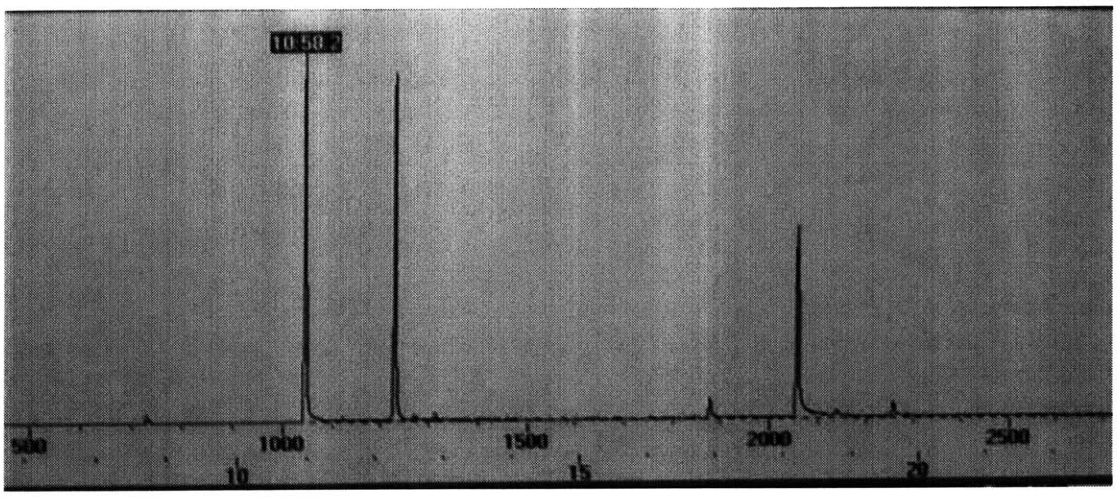

Picture 2-1 The chromatogram for a run of experimental sample 2.3. The elution times of the phosphate esters are: 10:58.2, 12:17.5 and 18:11.9 for TBP, TCEP and TBEP respectively

In order to have accurate results, injection standards were prepared with different concentrations of the phosphate esters in the same order of magnitude as the ones to be measured in the reaction samples. Three injection standards were prepared. Again, due to the need for precise knowledge of the concentration, micropipettes of 10 μL volume were used yielding standard concentrations of:

Table 2.3 Standards used

Standard	[TBP] μg/ml	[TCEP] μg/ml	[TBEP] μg/ml
1	97.7	134.8	94.6
2	48.9	67.4	47.3
3	9.8	13.4	9.5

The experimental samples analyzed in the GCMS were always bounded by injection standards to calibrate a response curve for each one of the phosphate esters.

2.4 Analysis and statistical manipulation of the GCMS results

Multiple GCMS analyses of the standards and the experimental samples were performed in a period of 3 weeks. Each GCMS injection lasted approximately 25 minutes. Since every time that GCMS injection took place the injection pattern consisted of injecting all standards followed by the experimental samples and re-injection of the standards (8 injections in total), each overall analysis required at least 4 hours. Frequently, the pattern described above was extended to analyze the experimental samples twice in the same day. Overall, 50 injections of standards and 27 of experimental samples were performed.

From the first injections it was clear that the GCMS yielded results with substantial variation. It was common for the same sample (standard or experimental) in consecutive runs to show a variation of 50% and in some occasions as high as a factor of 2. It was decided to deal with the uncertainty arising from this variation by multiple injections so that a result could be obtained with statistical methods. In the following tables (Table 2.4 & 2.5) the results of all the GCMS analyses are presented in their 'raw' form, without any manipulation.

Table 2.4 Results of GCMS analysis of standards

α/α	date	Standard #	selected ion	peak area	selected ion	peak area	Selected ion	peak area
			TBP		**TCEP**		**TBEP**	
1	20-Feb	1	99.3	2118347	63.2	831253	57.3	238537
2	20-Feb	2	99.3	944836	63.2	400739	57.3	100813
3	20-Feb	3	99.3	79882	63.2	49314	57.3	11652
4	20-Feb	2	99.3	798318	63.2	380932	57.3	90041
5	20-Feb	2	99.3	933681	63.2	432718	57.3	113879
6	23-Feb	1	99.3	2149166	63.2	1287168	57.3	255134
7	23-Feb	2	99.3	416566	63.2	325567	57.3	59350
8	23-Feb	3	99.3	35856	63.2	33000	57.3	7982
9	24-Feb	1	99.3	741439	63.2	560249	57.3	120608
10	24-Feb	2	99.3	265263	63.2	214923	57.3	47069
11	24-Feb	3	99.3	25401	63.2	21797	57.3	6940
12	24-Feb	3	99.3	27065	63.2	23400	57.3	7354
13	24-Feb	2	99.3	254842	63.2	209904	57.3	47573
14	24-Feb	1	99.3	931477	63.2	729610	57.3	144792
15	24-Feb	1	99.3	1340386	63.2	955607	57.3	195367
16	24-Feb	2	99.3	376675	63.2	308902	57.3	64111
17	24-Feb	3	99.3	30702	63.2	26136	57.3	8033
18	25-Feb	1	99.3	740099	63.2	634662	57.3	116819
19	25-Feb	2	99.3	259341	63.2	234867	57.3	47030
20	25-Feb	3	99.3	26628	63.2	21675	57.3	6802
21	25-Feb	1	99.3	1114352	63.2	823708	57.3	162202
22	25-Feb	2	99.3	343568	63.2	319206	57.3	63257
23	25-Feb	3	99.3	31636	63.2	30070	57.3	8250
24	25-Feb	1	99.3	1045023	63.2	799403	57.3	138754
25	25-Feb	1	99.3	1092066	63.2	847379	57.3	143794
26	25-Feb	2	99.3	419792	63.2	372737	57.3	68935
27	25-Feb	3	99.3	32679	63.2	30738	57.3	8648
28	27-Feb	1	99.3	995168	63.2	984984	57.3	178677
29	27-Feb	1	99.3	1393446	63.2	1098753	57.3	206875
29	27-Feb	1	99.3	1382146	63.2	1079203	57.3	207247
29	27-Feb	2	99.3	420532	63.2	411887	57.3	74741
29	27-Feb	3	99.3	43676	63.2	42654	57.3	12728

Table 2.4 continued

α/α	date	Standard #	selected ion	peak area	selected ion	peak area	Selected ion	peak area
			TBP		**TCEP**		**TBEP**	
30	1-Mar	1	99.3	2848398	63.2	1087902	57.3	373256
31	1-Mar	2	99.3	873119	63.2	478185	57.3	134240
32	1-Mar	3	99.3	82729	63.2	58396	57.3	11678
33	1-Mar	1	99.3	1918166	63.2	1104294	57.3	260421
34	1-Mar	2	99.3	606573	63.2	418221	57.3	244841
35	1-Mar	3	99.3	60600	63.2	49494	57.3	10982
36	2-Mar	1	99.3	763498	63.2	564566	57.3	115826
37	2-Mar	2	99.3	276481	63.2	231168	57.3	50653
38	2-Mar	3	99.3	27575	63.2	26313	57.3	7296
39	2-Mar	1	99.3	1506811	63.2	822382	57.3	227481
40	2-Mar	2	99.3	509327	63.2	303915	57.3	67877
41	2-Mar	3	99.3	48679	63.2	36776	57.3	10010
42	2-Mar	1	99.3	1018724	63.2	680438	57.3	167100
43	2-Mar	2	99.3	359402	63.2	285467	57.3	61211
44	2-Mar	3	99.3	30902	63.2	30847	57.3	8595
45	8-Mar	1	99.3	548469	63.2	266297	57.3	96055
46	8-Mar	2	99.3	215917	63.2	118332	57.3	41257
47	8-Mar	3	99.3	22146	63.2	13933	57.3	6717
48	8-Mar	1	99.3	724898	63.2	501027	57.3	139551
49	8-Mar	2	99.3	269687	63.2	189475	57.3	60374
50	8-Mar	3	99.3	25931	63.2	20210	57.3	8294

The best possible explanation of this systematic inconsistency in the GCMS analyses that we can provide is based on non-linear adsorption and desorption of the organic compounds in some regions of the GC column. This scenario implies that when the injection sample has a high concentration of organic compounds, more mass is adsorbed than is desorbed and that this mass is slowly released in the following injections. Of course this argument is highly speculative. In addition, the GCMS was used for many other experiments than the ones presented in this thesis which consisted of injecting highly concentrated natural organic matter (with concentrations orders of magnitude larger than the ones used in this set of experiments) that possibly compromised the sensitivity of the GCMS.

As it was mentioned before it was decided to perform numerous statistical analyses in order to interpret these measurements.

Table 2.5 Results of GCMS analysis of experimental samples

α/α	date	Experiment	selected ion	peak area	selected ion	peak area	selected ion	peak area
			TBP		TCEP		TBEP	
1	25-Feb	2.5	99.3	587498	63.2	540854	57.3	250666
2	25-Feb	2.1	99.3	319224	63.2	497686	57.3	123569
3	25-Feb	2.2	99.3	276676	63.2	477659	57.3	93760
4	25-Feb	2.3	99.3	280459	63.2	588051	57.3	92874
5	25-Feb	2.4	99.3	257734	63.2	557035	57.3	84156
6	27-Feb	2.5	99.3	577740	63.2	620810	57.3	329413
7	27-Feb	2.5	99.3	738244	63.2	732799	57.3	346099
8	1-Mar	2.5	99.3	1400840	63.2	808391	57.3	585531
9	1-Mar	2.1	99.3	743126	63.2	721658	57.3	251396
10	1-Mar	2.2	99.3	561925	63.2	656859	57.3	183297
11	1-Mar	2.3	99.3	523385	63.2	757176	57.3	167702
12	1-Mar	2.4	99.3	484312	63.2	706057	57.3	145367
13	2-Mar	2.5	99.3	480298	63.2	403382	57.3	232382
14	2-Mar	2.1	99.3	355017	63.2	512757	57.3	144738
15	2-Mar	2.2	99.3	704387	63.2	674644	57.3	286171
16	2-Mar	2.3	99.3	536126	63.2	659457	57.3	187322
17	2-Mar	2.4	99.3	518763	63.2	671608	57.3	160385
18	2-Mar	2.5	99.3	792411	63.2	549094	57.3	371655
19	2-Mar	2.1	99.3	389360	63.2	437625	57.3	143946
20	2-Mar	2.2	99.3	341802	63.2	459041	57.3	122091
21	2-Mar	2.3	99.3	294053	63.2	485931	57.3	101678
22	2-Mar	2.4	99.3	298703	63.2	510022	57.3	94952
23	8-Mar	2.5	99.3	398692	63.2	248553	57.3	213282
24	8-Mar	2.1	99.3	252057	63.2	275158	57.3	128380
25	8-Mar	2.2	99.3	226170	63.2	293649	57.3	98897
26	8-Mar	2.3	99.3	207352	63.2	321097	57.3	93712
27	8-Mar	2.4	99.3	187504	63.2	341608	57.3	85657

The injection of standards in the GCMS is intended to provide response curves for the selected phosphate esters. These response curves link the peak area of the selected ions measured from the mass spectrometer to a concentration of the selected compound.

Due to the inconsistency of the GCMS measurements, a response curve could not be established from single runs of the standards. Instead it was decided to generate an average response curve factor from all of the acceptable GCMS analyses of each standard (Table 2.6).

Table 2.6 Statistical values of GCMS results for standards

Standard 1			
	TBP	TCEP	TBEP
average	987,942	751,849	152,405
stdev	265,041	236,921	35,188
error %	26.8	31.5	23.1

Standard 2			
	TBP	TCEP	TBEP
average	314,682	263,352	56,928
stdev	71,592	85,586	10,728
error %	22.8	32.5	18.8

Standard 3			
	TBP	TCEP	TBEP
average	29,486	26,161	8,151
stdev	5,662	7,496	1,678
error %	19.2	28.7	20.6

The relative error in table (2.6) is calculated as $\frac{stdev}{average}$x100%. From table (2.6) it is evident that there is significant uncertainty in the calculated average values. It is also interesting the fact that the TCEP measurements show significantly greater uncertainty than the other two phosphate esters.

The error associated with the experimental samples measurements was higher than the one encountered in the standards. This time, TBP was the compound that showed the biggest inconsistency (Table 2.7).

Table 2.7 Statistical values of GCMS results for experimental samples

Experiments 2.5 (no reaction)			
	TBP	TCEP	TBEP
average	710,818	557,698	332,718
stdev	333,422	190,277	126,942
error %	47	34	38

Experiments 2.1			
	TBP	TCEP	TBEP
average	411,757	488,977	158,406
stdev	192,089	160,575	52,816
error %	47	33	33

Experiments 2.2			
	TBP	TCEP	TBEP
average	422,192	512,370	156,843
stdev	203,237	157,399	80,577
error %	48	31	51

Experiments 2.3			
	TBP	TCEP	TBEP
average	368,275	562,342	128,658
stdev	151,121	167,399	45,265
error %	41	30	35

Experiments 2.4			
	TBP	TCEP	TBEP
average	349,403	557,266	114,103
stdev	144,973	144,873	36,029
error %	41	26	32

Reaction rate constants and the relevant response curves

To derive the reaction rate constants from the experiments it is necessary to transform the mass spectrometer measurements to concentrations. This is accomplished using the response curves that translate the peak areas measured to concentrations.

It was decided to derive the response curves using two different techniques: one set of response curves would be generated from the average values of the standards and one would be generated using all the accepted runs of standards. For each of the two sets, the values would be plotted (area vs. concentration) and the curve with the best fit would be chosen.

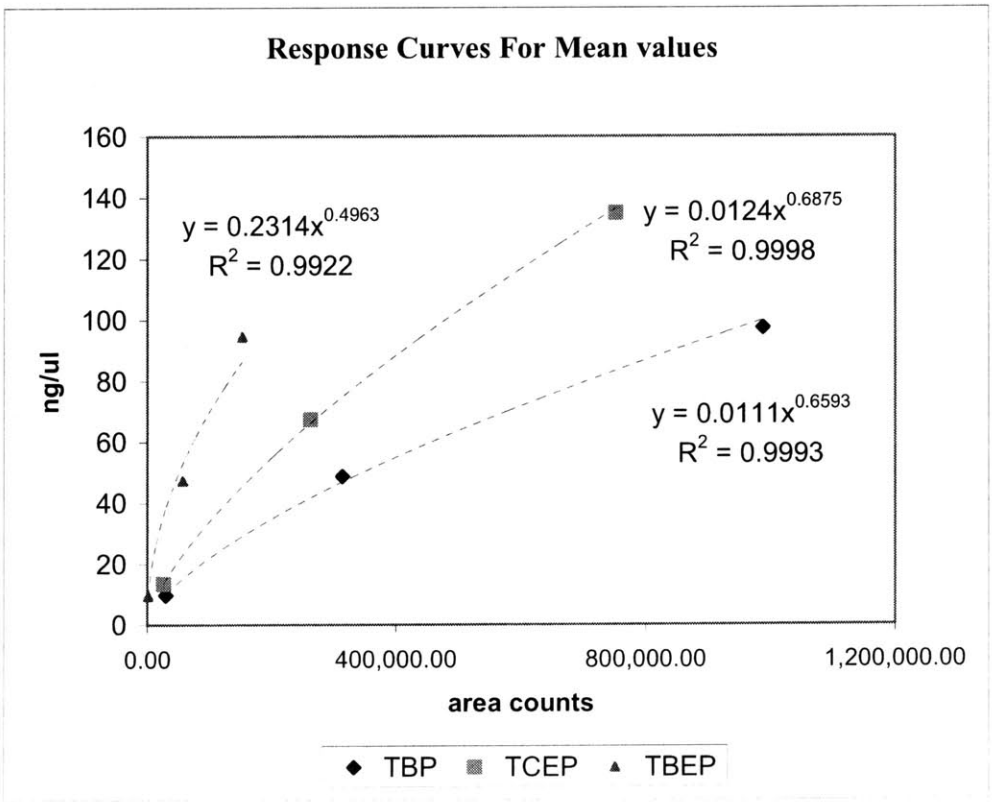

Figure 2-2

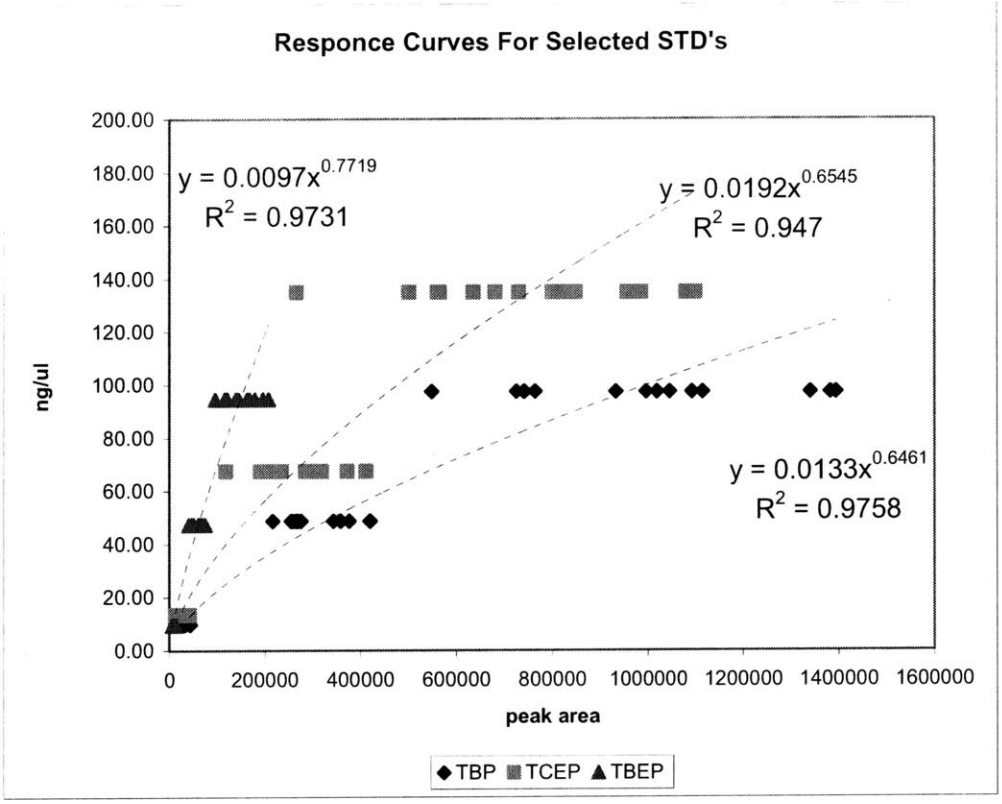

Figure 2-3

The best fit lines for both of the sets are power law curves and they all have very high values for R-squared. The response curve using only the mean values of the standards is (Figure 2-2):

$$\begin{aligned} C_{TBP} &= 0.011 \cdot (area)^{0.66} \\ C_{TCEP} &= 0.0124 \cdot (area)^{0.69} \\ C_{TBEP} &= 0.23 \cdot (area)^{0.5} \end{aligned} \qquad (2.11)$$

The response curve using all of the accepted standards is (Figure 2-3):

$$\begin{aligned} C_{TBP} &= 0.0133 \cdot (area)^{0.65} \\ C_{TCEP} &= 0.019 \cdot (area)^{0.655} \\ C_{TBEP} &= 0.01 \cdot (area)^{0.772} \end{aligned} \qquad (2.12)$$

Using the response factors, the mean values of peak area of the experimental samples and the samples volume the mass in the 50 ml sample was calculated.

Table 2.8 Mass in micrograms per 50 ml sample

Mass in micrograms per 50 ml sample

Using response curves from mean values

	TBP	TCEP	TBEP
EXPnr2	1,149.3	1,754.2	1,952.3
EXP2.1	840.8	1,617.9	1,421.6
EXP2.2	799.8	1,648.3	1,321.2
EXP2.3	656.1	1,551.3	1,091.8
EXP2.4	649.1	1,596.5	1,070.0

Using response curves from all STD's

	TBP	TCEP	TBEP
EXPnr2	1,156.4	1,760.5	2,580.8
EXP2.1	851.9	1,632.7	1,546.1
EXP2.2	812.0	1,666.1	1,340.0
EXP2.3	666.8	1,561.5	1,080.9
EXP2.4	660.1	1,606.5	1,034.8

From table 2.8 it is obvious that the different response curves used give approximately analogous results with the sole exception of mass of TBEP for the experimental sample without the Fenton reaction. This difference is expected to alter significantly the reaction rate constants that will be obtained for TBEP for each set of response curves.

The mass per 50 ml sample was translated to concentration and the competition method was used to derive the reaction rate from each sample's data.

The reaction rate constants that are derived are:

Table 2.9 Reaction Rate Constants (response factors from mean STD's values)

Experiment	kTCEP [$M^{-1}s^{-1}$]	kTBEP [$M^{-1}s^{-1}$]
2.1	2.6E+09	1.0E+10
2.2	1.7E+09	1.1E+10
2.3	2.2E+09	1.0E+10
2.4	1.6E+09	1.1E+10
Regression	~1.5E+09	~1.0E+10

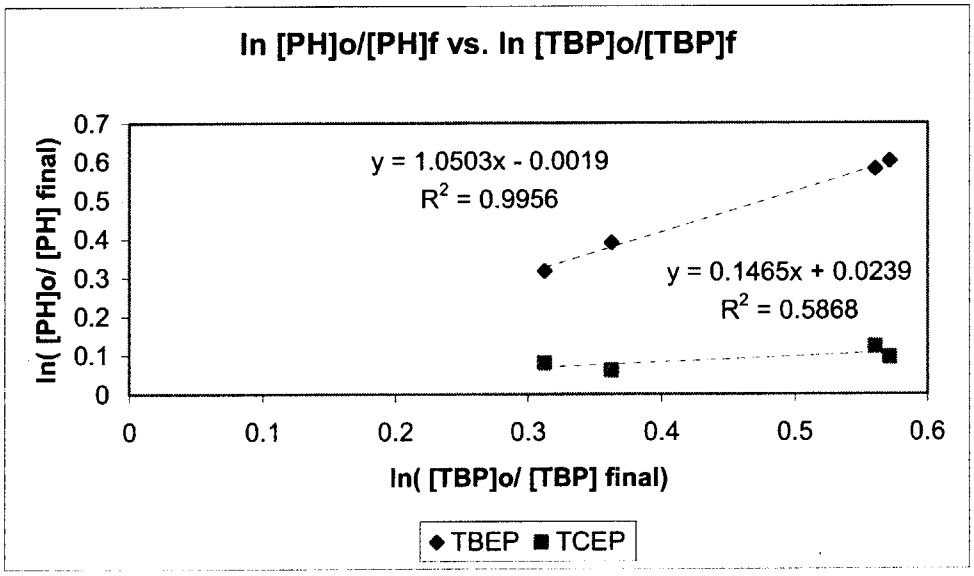

Figure 2-4 Response factors from mean STD's values

Using the response factors derived from the mean values of the standards.

Table 2.10 Rate Constants (response factors from all accepted STD's values)

Experiment	kTCEP [$M^{-1}s^{-1}$]	kTBEP [$M^{-1}s^{-1}$]
2.1	2.5E+09	1.7E+10
2.2	1.6E+09	1.9E+10
2.3	2.2E+09	1.6E+10
2.4	1.6E+09	1.6E+10

Regression	~1.6E+09	1.4E+10

Using the response factors derived from all of the accepted standards.

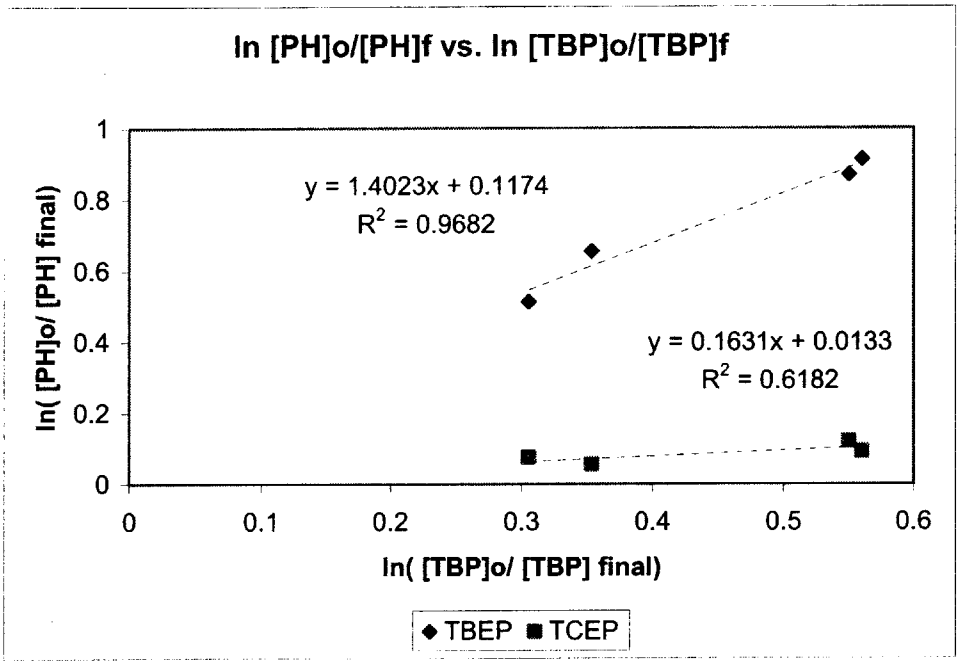

Figure 2-5 Response factors from all accepted STD's values

From tables 2.9 & 2.10 it is obvious that the derived reaction rate constants vary from experiment to experiment based on the response curves used. It is evident that TCEP is reacting significantly more slowly than TBP and TBEP slightly faster than TBP. The problem with the derived rate constants is that with the method used, we cannot do error propagations to estimate confidence intervals. In tables 2.6 & 2.7 the statistical values of the standards and experimental samples are given. The error of the mean values is very high, which implies that the derived rate constants might be compromised by that. It is therefore necessary to derive error estimates for the values of the rate constants

2.5 A probabilistic approach for the rate constants

The reason why we cannot associate error to the rate constants derived with the method described above is that even though the uncertainty in each individual step (GCMS results) is known, its propagation through the response curves and the ensuing calculations is not clear.

A widely used method that incorporates a probabilistic approach and acknowledges the propagation of error in complicated calculations is the Monte Carlo simulation method. This method is based on the assumption that all the physical quantities involved in the calculation steps follow a known and well defined statistical distribution. For example, in the case of the GCMS results, this assumption implies that every result for a given sample is but one of the possible realizations that the GCMS gives for the injected mass. The fundamental idea behind this method is that our measurements have some inherent uncertainty associated with them.

The solution that Monte Carlo simulation proposes is a trial method. If we repeat our experiment for a large number of times, the standard deviation of our results will be close to the actual value.

The way that the method is implemented for the GCMS results is by assuming that they follow a known statistical distribution. In this work, it was assumed that they follow a Gaussian distribution since there was not any evidence implying something different. A set of random numbers in the range of 0 to 1 was created. From the statistical manipulation of the GCMS results, the estimate of the mean value and the standard deviation for every standard and experimental sample was known. Using the set of random numbers and the statistical facts for the GCMS samples we can create a set of new GCMS results by assigning their value to be the inverse value of the Gaussian distribution that has the known mean and standard deviation with the probability of the random number.

Following the method described above, a statistically consistent set of 1000 values for every standard and every experimental sample was created for each chemical. From each triplet of standards, a linear response curve was derived (Excel can only perform automatically linear regression with the functions slope and intercept). Using this unique response factor the mass for each sample and consequently the molar

concentration was calculated. As a result of these calculations, a mean value and a standard deviation for the molar concentration of TBP, TCEP and TBEP for every experimental sample was calculated.

Using again the set of random numbers and the mean and variance of the molar concentrations, a set of a thousand experiments was simulated. This set of experiments had the same probability associated with every step for each experiment. The reaction rate for each compound was calculated using the competition method for each of the simulated experiments. Following this methodology, a set of 4*1000 reaction rate constants, statistically consistent, were obtained for TCEP and TBEP. In this set of reaction rate constants, descriptive statistics were then applied to obtain the mean reaction rate constants and the 90% confidence interval.

At this point it must be mentioned that some form of inconsistency exists even in the Monte Carlo method. This comes from the fact that when the set of a thousand experiments was simulated some of the values of the random probabilities used resulted in negative concentrations in the experimental samples. Since there is no correct way to deal with this problem it was decided to use the absolute values of concentrations. A similar problem also appeared when the rate constants were calculated; some of the random probabilities resulted in negative rate constants. These rate constants were discarded. It is clear that this artificial "correction" of the values introduces error in the performed simulation. This introduced error is expected to affect the final results and especially the reaction rate constants calculated at the end. It is the researcher's belief that the error will be more associated with the mean value of the reaction rate constant than the estimate of the uncertainty which is our goal when performing this simulation.

The final result obtained by the Monte Carlo simulation are presented in the following tables, which are printouts from applying the descriptive statistics tool from Excel to the set of reaction rate constants created.

Table 2.11 Descriptive Statistics for the rate constant of TCEP

K TCEP	
Mean	**3.2E+09**
Standard Error	3.7E+08
Median	**1.1E+09**
Mode	
Standard Deviation	1.9E+10
Sample Variance	3.8E+20
Kurtosis	578.15
Skewness	21.66
Range	6.1E+11
Minimum	8.4E+05
Maximum	6.1E+11
Sum	8.7E+12
Count	2713
Confidence Level(90.0%)	**6.1E+08**

Table 2.12 Descriptive Statistics for the rate constant of TBEP

K TBEP	
Mean	**3.1E+10**
Standard Error	3.3E+09
Median	**1.4E+10**
Mode	
Standard Deviation	2.1E+11
Sample Variance	4.2E+22
Kurtosis	944.48
Skewness	28.28
Range	7.9E+12
Minimum	1.4E+09
Maximum	7.9E+12
Sum	1.2E+14
Count	3814
Confidence Level(90.0%)	**5.5E+09**

2.6 Experimentally derived rate constants

The Monte Carlo simulation suggests that the rate constants for TCEP and TBEP are:

kTCEP = $3.2 \cdot 10^{9}$ $M^{-1}s^{-1}$ with a 90% confidence interval of $6.1 \cdot 10^{8}$ $M^{-1}s^{-1}$

and

kTBEP = $3.1 \cdot 10^{10}$ $M^{-1}s^{-1}$ with a 90% confidence interval of $5.5 \cdot 10^{9}$ $M^{-1}s^{-1}$

These values are slightly higher from the ones calculated using the simple statistical method. From tables 2.11 & 2.12 it is evident that the calculated rate constants do not follow a perfect Gaussian distribution.

Taking into account both methods used to derive the rate constants and the small inconsistencies in the Monte Carlo simulation method (which we expect to give a higher reaction rate than the actual one), an estimate of the rate constants of TCEP and TBEP with hydroxyl radical that is proposed from the experimental values is:

kTCEP = $2 \cdot 10^{9}$ $M^{-1}s^{-1}$ with a 90% confidence interval of approximately $1 \cdot 10^{9}$ $M^{-1}s^{-1}$

and

kTBEP = $2 \cdot 10^{10}$ $M^{-1}s^{-1}$ with a 90% confidence interval of approximately $1 \cdot 10^{10}$ $M^{-1}s^{-1}$

Due to the uncertainty that the experiments had, a detailed discussion of the rate constants from a theoretical point of view follows

3 A theoretical approach for the rate constants of the phosphate esters with hydroxyl radical

From the analysis of the experimental results and the methods used to derive the rate constants it is obvious that there is some intrinsic uncertainty to the results. Because the precise knowledge of the rate constants of TCEP and TBEP with hydroxyl radical is essential for the rest of this thesis, a theoretical approach will be used to evaluate the plausibility of the experimentally derived constants. The theoretical approach consists of applying the encounter theory to the phosphate esters in question and taking into account the possible effects that their structure might have on the rate constants with hydroxyl radical.

3.1 Determining upper limits for the reaction rate constants of the phosphate esters with hydroxyl radical

For very fast chemical reactions like ones in which hydroxyl radical is a reactant, an upper limit for the rate constants can be set by the encounter theory. The encounter theory states that the rates of these reactions are limited by the molecular collision frequency. An upper limit on molecular collision frequency is set by molecular diffusion and can be described by the Smoluchowski – Debye theory.

From Stumm and Morgan (1996), the equation for diffusion-controlled rate constant ($M^{-1}s^{-1}$) is

$$k_E = \frac{4\pi N}{1000}(D_A + D_B)(r_A + r_B)f \qquad (3.1)$$

where N is Avogadro's number, D is the diffusion coefficient (cm^2s^{-1}), r the solute species radius (cm) and f a factor that accounts for long range forces (electrostatic effects).

Equation (3.1) will be used to calculate the diffusion-controlled rate constants for the phosphate esters reactions with hydroxyl radical. The required values of molecular diffusivity and solute species radii will be estimated with the method presented by

Schwarzenbach, Gschwend and Imboden (2003). Also it has to be noted that f is equal to 1 since hydroxyl is a neutral species.

Solute Species molecular diffusivities and radii

For hydroxyl radical $(OH\bullet)$ Buxton et al. (1988) give the following values for molecular radius and diffusion coefficient:

$$r_{OH\bullet} = 2.2 \cdot 10^{-8} cm \text{ and } D_{OH\bullet} = 2.3 \cdot 10^{-5} cm^2 s^{-1}$$

For the phosphate esters the molecular radius can be estimated from their molecular weight and their liquid density, assuming that the molecules are spherical.

$$r = \left[\frac{3 \frac{MW}{\rho_L}}{4\pi N} \right]^{1/3} \qquad (3.2)$$

The molecular diffusion coefficients can be estimated from their molar mass from the following relationship given by Schwarzenbach, Gschwend and Imboden (2003):

$$D_w = \frac{2.4 \cdot 10^{-4}}{MW^{0.71}} \ (\text{cm}^2\text{s}^{-1}) \qquad (3.3)$$

Using the previous equations and the physical data for the phosphate esters, the following radii, molecular diffusion coefficients and rate constant can be estimated:

Table 3.1 Phosphate Esters Molecular radii, diffusion coefficients and rate constants

	Molecular radius (cm)	**Molecular diffusion** (cm^2s^{-1})	**Rate Constant** ($M^{-1}s^{-1}$)
TBP	$4.8 \cdot 10^{-8}$	$5.1 \cdot 10^{-6}$	$1.5 \cdot 10^{10}$
TCEP	$4.3 \cdot 10^{-8}$	$4.9 \cdot 10^{-6}$	$1.4 \cdot 10^{10}$
TBEP	$5.4 \cdot 10^{-8}$	$3.8 \cdot 10^{-6}$	$1.5 \cdot 10^{10}$

3.2 Effects of structure of the phosphate esters on their reaction rate constants

The three phosphate esters in question have similar physical characteristics but their small differences in structure might have a substantial effect on their reaction rate constants with hydroxyl radical.

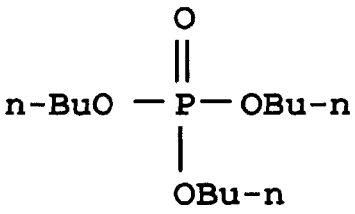

Figure 3-1 **Structure of TBP, Molecular formula $C_{12}H_{27}O_4P$**

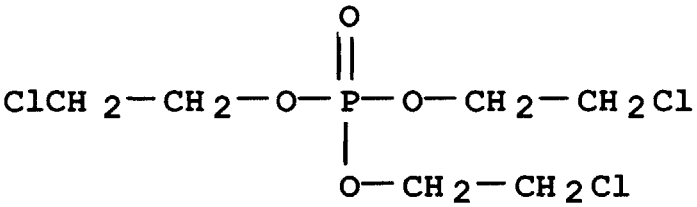

Figure 3-2 **Structure of TCEP, Molecular formula $C_6H_{12}Cl_3O_4P$**

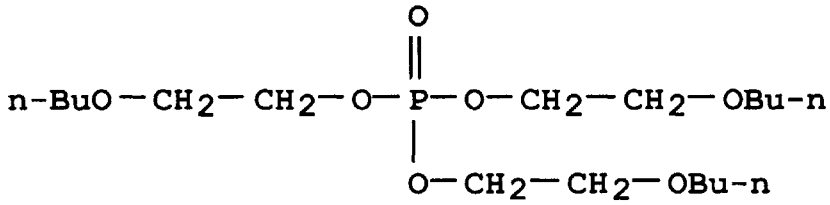

Figure 3-3 **Structure of TBEP, Molecular formula $C_{18}H_{39}O_7P$**

Hydroxyl radical is known to react mainly via three different mechanisms with organic compounds in aqueous solutions (Masschelein, 2002). These mechanisms are:

- Hydrogen atom abstraction
- Electrophilic addition to carbon bonds
- Electron transfer reactions

Of these mechanisms, the first two are generally considered the most important.

Since TBP, TBEP and TCEP all have completely saturated carbon bonds, the main mechanism of reaction with hydroxyl radical is hydrogen abstraction.

Effect of size

It can be argued that when a molecule has more hydrogen atoms readily available for abstraction, it will react faster with hydroxyl radical. This can be attributed to the fact that more collisions in such a molecule will be successful than in a molecule with fewer available hydrogen atoms. From Table 3.2 we can observe that the rate constants of hydroxyl radical with selected alkanes decreases with decreasing number of available hydrogen atoms.

Based on this observation it is expected that the rate constants of the phosphate esters will follow the pattern:

$$k_{TBEP} > k_{TBP} > k_{TCEP}$$

Table 3.2 Rate constants of various compounds from Notre Dame Radiation Laboratory

Compound		Rate Constant (M-1s-1)
Pentane	CH3-CH2-CH2-CH2-CH3	$5.4 \cdot 10^9$
Butane	CH3-CH2-CH2-CH3	$2.9 \cdot 10^9$
Propane	CH3-CH2-CH3	$2.3 \cdot 10^9$
Ethane	CH3-CH3	$1.4 \cdot 10^9$
Methane	CH4	$1.2 \cdot 10^8$
Ethanol	CH3-CH2-OH	$1.9 \cdot 10^9$
2-Chloroethanol	Cl-CH2-CH2-OH	$9.5 \cdot 10^8$

Effect of the Chlorine atoms in TCEP

The presence of the three chlorine atoms at the end of the carbon chains in TCEP is expected to affect the reaction rate of TCEP with hydroxyl radical.

Chlorine atoms are highly electronegative, making hydrogen abstraction less feasible. In addition, according to the suggested reaction mechanisms a number of collisions will result in electron transfer reactions:

$$OH\bullet + RX \rightarrow OH^- + RX^{+\bullet}$$

$RX^{+\bullet}$ is some form of radical but it is probable that it does not initiate other reactions than the back reaction with hydroxyl radical. Therefore this mechanism might not lead to successful collisions.

These effects of chlorine atoms have been studied in more depth in the gas phase, where structure-reactivity models have been proposed for estimating the reaction rate constants of organic compounds with hydroxyl radicals. Schwarzenbach, Gschwend and Imboden (2003) present a model in which the substitution of a chlorine atom (group substituent $-CH_2Cl$) results in a decrease of the reaction rate for hydrogen abstraction by a factor of 0.36. In TCEP three such groups are present. Therefore the above model, which cannot be readily extended for aqueous solutions, predicts a significant decrease of the reaction rate.

In Table 3.2 data are presented for the rate constants of Ethanol and 2-Chloroethanol that show this decrease. The decrease is a factor of 0.5.

Conclusion

Based on all the previous arguments and assuming that the effects are additive (they might even be multiplicative), a reasonable expectation would be that the reaction rate constants of the phosphate esters will follow the pattern $k_{TBEP} > k_{TBP} >> k_{TCEP}$. It is not expected that TBEP and TBP react at significantly different rates, but for TCEP a slower reaction rate of an order of magnitude would seem reasonable.

3.3 Discussion on reaction rate constants and closure

It is evident that in general the experimentally derived rate constants agree well with the theoretical predictions. Taking into account all of the previous analyses, the following rate constants are proposed for the reactions of TCEP and TBEP with hydroxyl radical:

$$k\text{TCEP} = 2 \cdot 10^{9}\ \text{M}^{-1}\text{s}^{-1} \qquad (3.4)$$

and

$$k\text{TBEP} = 2 \cdot 10^{10}\ \text{M}^{-1}\text{s}^{-1} \qquad (3.5)$$

4 The H_2O_2/UV oxidation process

The elementary reactions of H_2O_2 photolysis

From investigations of hydrogen peroxide photolysis it is indicated that radical chain reactions occur in a hydrogen peroxide solution under UV light irradiation. According to the mechanism of the H_2O_2/UV oxidation process presented by Crittenden et al. (1999) the following reactions take place.

Initiation: (primary photolysis of H_2O_2 or HO_2^-)

$$H_2O_2 / HO_2^- + h\nu \rightarrow 2OH\bullet \qquad (4.1)$$

Propagation:

$$H_2O_2/HO_2^- + OH\bullet \rightarrow H_2O/OH^- + HO_2 \qquad (4.2)$$

$$H_2O_2 + HO_2/O_2 \rightarrow OH\bullet + H_2O/OH^- + O_2 \qquad (4.3)$$

Termination:

$$OH\bullet + OH\bullet \rightarrow H_2O_2 \qquad (4.4)$$

$$HO + HO_2\bullet/O_2\bullet^- \rightarrow H_2O/OH^- + O_2 \qquad (4.5)$$

$$HO_2 + HO_2\bullet/O_2\bullet^- \rightarrow H_2O_2/HO_2^- + O_2 \qquad (4.6)$$

Although the primary quantum (Φp) of the hydrogen peroxide photolysis reaction (4.1) is at 254 nm 0.5, due to reaction (4.5) the overall quantum yield (Φ_T) of hydrogen peroxide in the above reaction mechanism is 1.

Other species of significance

There is a great variety of naturally occurring species in unpurified water that act as hydroxyl radical scavengers to reduce the oxidation efficiency of any AOP. The most important inorganic hydroxyl radical scavengers in natural waters are the carbonate and bicarbonate ions. Carbonate and bicarbonate ions (CO_3^{2-}/HCO_3^-) react with hydroxyl radicals to produce carbonate radicals ($CO_3^-\bullet/HCO_3\bullet$) which are equally active. The carbonate radicals react with hydrogen peroxide to form superoxide radicals ($HO_2\bullet$). It is

important to note that the carbonate ion is a much more active hydroxyl radical scavenger than bicarbonate ion (the reaction rate for bicarbonate ion is two orders of magnitude larger than for the carbonate ion). Therefore the solution pH affects the hydroxyl radical concentration.

Kinetic Rates

Based on the above mechanism for the H_2O_2/UV AOP the kinetic rate expressions can be written for the species of interest which are:

H_2O_2/HO_2^- , OH• , HO_2•/O_2^-• , CO_3^-• , CO_3^{2-}/HCO_3^- and the target organic compounds TBP, TCEP and TBEP

$$\begin{aligned} r_{H_2O_2/HO_2^-} = r_{UV,H_2O_2}(-k_1[H_2O_2]) - k_2[H_2O_2][OH\bullet] - k_3[HO_2^-][OH\bullet] \\ -k_4[H_2O_2][HO_2\bullet] - k_5[H_2O_2][O_2^-\bullet] - k_8[H_2O_2][CO_3^-\bullet] \\ -k_9[HO_2^-][CO_3^-\bullet] + k_{10}[OH\bullet][OH\bullet] \\ +k_{12}[HO_2\bullet][HO_2\bullet] + k_{13}[HO_2\bullet][O_2^-\bullet] \end{aligned} \quad (4.7)$$

$$\begin{aligned} r_{OH\bullet} = r_{UV,OH\bullet}(+2k_1[H_2O_2]) - k_2[H_2O_2][OH\bullet] - k_3[HO_2^-][OH\bullet] \\ +k_4[H_2O_2][HO_2\bullet] + k_5[H_2O_2][O_2^-\bullet] \\ -k_6[OH\bullet][CO_3^{2-}] - k_7[OH\bullet][HCO_3^-] \\ -k_{10}[OH\bullet][OH\bullet] - k_{11}[OH\bullet][HO_2\bullet] \\ -k_{14}[OH\bullet][O_2^-\bullet] - k_{15}[OH\bullet][CO_3^{2-}\bullet] \\ -k_{TBP}[OH\bullet][TBP] - k_{TCEP}[OH\bullet][TCEP] - k_{TBEP}[OH\bullet][TBEP] \end{aligned} \quad (4.8)$$

$$
\begin{aligned}
r_{HO_2\bullet/O_2^-\bullet} = {} & k_2[H_2O_2][OH\bullet] + k_3[HO_2^-][OH\bullet] - k_4[HO_2\bullet][H_2O_2] \\
& - k_5[O_2^-\bullet][H_2O_2] + k_8[H_2O_2][CO_3^-\bullet] + k_9[CO_3^-\bullet][HO_2^-] \\
& - k_{11}[HO_2\bullet][OH\bullet] - k_{12}[HO_2\bullet][HO_2\bullet] - k_{13}[HO_2\bullet][O_2^-\bullet] \\
& - k_{14}[O_2^-\bullet][OH\bullet] - k_{16}[O_2^-\bullet][CO_3^-\bullet]
\end{aligned} \tag{4.9}
$$

$$
\begin{aligned}
r_{CO_3^-\bullet} = {} & k_6[OH\bullet][CO_3^{2-}] + k_7[OH\bullet][HCO_3^-] \\
& - k_8[CO_3^-\bullet][H_2O_2] - k_9[CO_3^-\bullet][HO_2^-] \\
& - k_{15}[CO_3^-\bullet][OH\bullet] - k_{16}[CO_3^-\bullet][O_2^-\bullet] \\
& - k_{17}[CO_3^-\bullet][CO_3^-\bullet]
\end{aligned} \tag{4.10}
$$

$$
\begin{aligned}
r_{CO_3^{2-}/HCO_3^-} = {} & -k_6[CO_3^{2-}][OH\bullet] - k_7[HCO_3^-][OH\bullet] \\
& + k_8[CO_3^-\bullet][H_2O_2] + k_9[CO_3^-\bullet][HO_2^-] \\
& + k_{17}[CO_3^-\bullet][O_2^-\bullet]
\end{aligned} \tag{4.11}
$$

For the oxidation of the target phosphate esters (TBP, TCEP and TBEP) in the current model it has been assumed that they only react with hydroxyl radical. It is possible that the phosphate esters react with the other radicals that are created and that they have various oxidation steps prior to being completely mineralized. All these steps will be neglected since there is no knowledge of the exact products.

Therefore the reaction rate constants for the phosphate esters are:

$$
\begin{aligned}
r_{TBP} &= -k_{TBP}[OH\bullet][TBP] \\
r_{TCEP} &= -k_{TCEP}[OH\bullet][TCEP] \\
r_{TBEP} &= -k_{TBEP}[OH\bullet][TBEP]
\end{aligned} \tag{4.12}
$$

Table 4.1 The elementary reactions in a H_2O_2/UV AOP system

No.	Reactions	Rate constants, $M^{-1}s^{-1}$
1	$H_2O_2 / HO_2^- + h\nu \rightarrow 2OH\bullet$	$r_{UV,H_2O_2} = -\Phi_{H_2O_2} I_o f_{H_2O_2} (1-e^{-A})$
2	$H_2O_2 + OH\bullet \rightarrow H_2O + HO_2\bullet$	$k_2 = 2.7\times10^7$
3	$OH\bullet + HO_2^- \rightarrow HO_2\bullet + OH^-$	$k_3 = 7.5\times10^9$
4	$H_2O_2 + HO_2\bullet \rightarrow OH\bullet + H_2O + O_2$	$k_4 = 3$
5	$H_2O_2 + O_2^-\bullet \rightarrow OH\bullet + O_2 + OH^-$	$k_5 = 0.13$
6	$OH\bullet + CO_3^{2-} \rightarrow CO_3^-\bullet + OH^-$	$k_6 = 3.9\times10^8$
7	$OH\bullet + HCO_3^- \rightarrow CO_3^-\bullet + H_2O$	$k_7 = 8.5\times10^6$
8	$H_2O_2 + CO_3^-\bullet \rightarrow HCO_3^- + HO_2\bullet$	$k_8 = 4.3\times10^5$
9	$HO_2^- + CO_3^-\bullet \rightarrow CO_3^{2-} + HO_2\bullet$	$k_9 = 3.0\times10^7$
10	$OH\bullet + OH\bullet \rightarrow H_2O_2$	$k_{10} = 5.5\times10^9$
11	$OH\bullet + HO_2\bullet \rightarrow H_2O + O_2$	$k_{11} = 6.6\times10^9$
12	$HO_2\bullet + HO_2\bullet \rightarrow H_2O_2 + O_2$	$k_{12} = 8.3\times10^5$
13	$HO_2\bullet + O_2^-\bullet \rightarrow HO_2^- + O_2$	$k_{13} = 9.7\times10^7$
14	$OH\bullet + O_2^-\bullet \rightarrow O_2 + OH^-$	$k_{14} = 7.0\times10^9$
15	$OH\bullet + CO_3^-\bullet \rightarrow ?$	$k_{15} = 3.0\times10^9$
16	$CO_3^-\bullet + O_2^-\bullet \rightarrow CO_3^{2-} + O_2$	$k_{16} = 6.0\times10^8$
17	$CO_3^-\bullet + CO_3^-\bullet \rightarrow ?$	$k_{17} = 3.0\times10^7$
18	$H_2CO_3^* \rightleftharpoons H^+ + HCO_3^-$	$pK_{a1} = 6.3$
19	$HCO_3^- \rightleftharpoons H^+ + CO_3^{2-}$	$pK_{a2} = 10.3$
20	$H_2O_2 \rightleftharpoons H^+ + HO_2^-$	$pK_{a5} = 11.6$
21	$HO_2A \rightleftharpoons H^+ + O_2A^-$	$pK_{a6} = 4.8$

The values come from Crittenden et al. (1999)

4.1 Conceptual model of the ultra violet disinfection unit

The disinfection process that is considered for implementing an Advanced Oxidation Process for the removal of the phosphate esters from drinking water is ultraviolet disinfection.

Ultraviolet disinfection units usually consist of flow through reactors with an exposure to almost homogeneous light intensities for a small period of time (less than one minute in most designs). These reactors are designed to achieve the least dispersive behavior trying to mimic a plug flow reactor. Therefore for the purposes of this thesis they can be modeled as one.

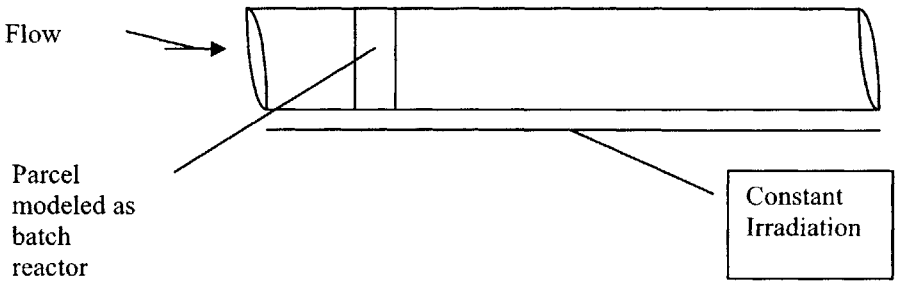

Schematic of a UV disinfection reactor

The steady state equation for conservation of mass in a plug flow reactor is

$$U\frac{dC}{dx} = \sum \text{sources} - \sum \text{sinks} \quad (4.13)$$

Assuming a moving coordinate system, $x = Ut$ and using the chain rule of differentiation the equation transforms to

$$\frac{dC}{dt} = \sum \text{sources} - \sum \text{sinks} \quad (4.14)$$

The equation now corresponds to the time domain and not the spatial domain and essentially tracks a parcel of water that enters the reactor.

The parcel of water entering this reactor is advected while experiencing homogeneous ultraviolet irradiation. Equation (4.14) implies that the degradation of pollutant for this parcel of water can be modeled as a batch reactor process since due to absence of dispersion it does not mix with the surrounding water. For this parcel the reaction time is equal to the hydraulic residence time $\tau = \frac{L}{V}$. The governing equation derived from mass conservation is (4.14), where sources and sinks refer to the various chemical reactions taking place in the parcel.

4.2 Characteristics of our ideal UV reactor

The first documented large-scale application of UV disinfection systems for drinking water is in Marseille, France from 1906-1909 (Masschelein 2002). Since then the application of UV light for disinfection and other treatments of water, wastewater and industrial effluents has grown significantly. As a consequence, specialized companies have appeared that offer compact off-the-shelf solutions to various engineering needs. These companies have accumulated substantial knowledge of the various design factors and have been involved in extensive research. As a result they offer proprietary technology and they are involved in the design procedure of every UV installation, offering expert consulting services.

The exact characteristics of all of these UV disinfection units are not publicly available and even if they were, there are so many competing designs that one cannot be chosen without considering other attributes, such as the economic cost or the proximity of the manufacturer. Berson-UV, Wedeco and Trojan Technologies are only a few of the leading manufacturers of UV units. For the goals of the present thesis, it has been decided to use an "ideal" reactor.

The first consideration about a UV disinfection unit is its germicidal efficiency. Because this is a matter of public health, government agencies around the world have developed regulations specifying the minimum UV irradiation dose that each UV disinfection unit must provide. Here we will follow the Austrian regulations, which require a UV irradiation dose of 400 J/m^2.

It has to be noted that in everything that follows we are only considering light with a wavelength of 254 nm.

Following the description of a UV reactor as a plug flow reactor, we will assume the simplest design, a cylindrical reactor with a length of 2 m and a diameter of 1 m with one lamp in the center. In addition we will assume that the hydraulic residence time in the

reactor is 20 sec. This leads to a mean velocity for water of 0.1 m/sec and a flow rate of 282.74 m^3/hour.

The light intensity inside the reactor is not homogeneous. As the light travels away from the source it is attenuated. This happens due to two mechanisms, dissipation and absorption. Dissipation is the effect of the increasing area in which the energy is projected away from the source, and the effect can be calculated as follows:

$$I=\frac{S}{2\pi d^2} \qquad (4.15)$$

where S is the power of the light source (Watts) and d the distance from the source (cm) and I the intensity (Watts/cm^2).

Absorption is described by Beer's law which relates the attenuation to the absorptive properties of the medium through which the light travels.

$$I=Io\cdot e^{-A\cdot d} \qquad (4.16)$$

where A is the absorbance of the solution (cm^{-1}) and d the length of the absorbing media (cm).

Combining both attenuation processes we can derive an expression describing the intensity at any point away from a single source.

$$I=\frac{S}{2\pi d^2}\cdot e^{-A\cdot d} \qquad (4.17)$$

where the intensity is given as power per unit area (Watts/cm^2).

The lamp in the UV reactor is a line source that can be approximated as a series of point sources. This method is called point source summation and the reader is referred to the EPA's Design Manual for Municipal Wastewater Disinfection for a complete description. The Figure 4-1 shows the basis of the method.

The equation governing the light intensity at any given point in the reactor is:

$$I(r,z_o) = \sum_{n=1}^{n=N} \frac{S/N}{4\pi(r^2+z_n^{\,2})} \cdot e^{-A\cdot\sqrt{r^2+z_n^{\,2}}} \qquad (4.18)$$

$$\text{with } z_n = z_o - L(n/N)$$

where N is the number of point sources that the UV lamp is approximated by, L the length of the UV lamp, r and zo are the radial distance and the z coordinate respectively of the point for which we are calculating the intensity from the UV lamp. Zn is a relative distance defined in Figure 4-1.

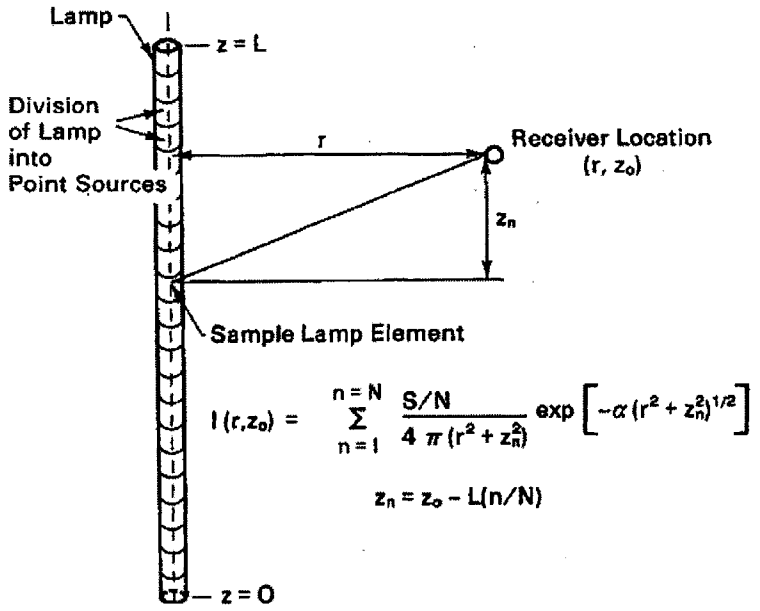

Figure 4-1 Point Source Summation from Design Manual: Municipal Wastewater Disinfection

The required intensity can be evaluated based on the assumption of plug flow. In a plug flow reactor flow lines are straight. We must design the reactor with a sufficiently high intensity to satisfy the exposure dose requirement even for the flow line of minimum intensity.

In a reactor with one UV lamp in the center, the minimum intensity flow lines are the ones in the perimeter of the circle (r = 50 cm). Using the point source summation technique we can calculate the required power of the lamp to realize the exposure dose

for these flow lines. The absorbance of the solution needs to be defined first. Following suggestions of Masschelein, (2002) we will assume an absorbance of 0.02 cm^{-1}. (see further discussion in chapter 4.3)

The dose of UV radiation for any particle traveling along a flow line can be defined as $D=\bar{I}\times t^*$ where t* is the residence time in the reactor and $\bar{I}$ the average light intensity along the flow line. The average light intensity along the flow line can be calculated using the point source summation method: the intensity is calculated for a number of points in the flow line Zo, and the average is found by summing the calculated intensities and dividing by the number of calculation points. Since we are trying to find the necessary power of the lamp we use the point source summation assuming a power source of 1 Watt. To realize the necessary exposure dose the source needs to emit the following power:

$$S=\frac{D(J/cm^2)}{f(\text{geometry,absorbance})\,(cm^2)\cdot t^*(sec)}\ (J/sec=Watts) \quad (4.19)$$

where D is the exposure dose and f the result of the calculation of the average light intensity along the flow line of minimum intensity for a light source of power 1 Watt.

For the characteristics of our reactor (geometric factors and properties of the solution) the required power of the lamp is $S \sim 459$ Watt.

The units must be converted to einsteins since this is the unit associated with the quantum yield of the compounds. One einstein (ein) is the energy equivalent of 1 mole of photons at a specified wavelength. For the wavelength of 254 nm the energy of 1 einstein is $E=Ne\cdot h\cdot\frac{c}{\lambda}=6\cdot10^{23}\cdot6.63\cdot10^{-34}\cdot\frac{3\cdot10^{8}}{254\cdot10^{-9}}J\approx469842.5J$. Therefore the necessary power of the lamp in einsteins per second is: $S\approx9.77\cdot10^{-4}$ ein/sec.

Our ideal UV reactor has been fully defined based on the necessary UV dose. The chosen characteristics are:

Table 4.2 Ideal UV reactor's characteristics

Length	L	2 m
Diameter	D	1 m
Hydraulic residence time	t*	20 sec
Mean velocity	V	0.1 m/sec
Flow rate	Q	282.74 m^3/hour
Exposure dose	D	400 J/m^2
Power output of lamp	S	459 Watt ~ 0.000977 ein/sec

4.3 Implementing the model of H_2O_2/UV advanced oxidation process

The mechanisms of the oxidation process, the conceptual model of the disinfection tank and the characteristics of our ideal UV reactor have been previously defined. To be able to produce a kinetic model for the process we must now define the overall problem from a chemical point of view.

The overall reaction rate constants for the species participating in the process have been formulated in such a way as to correspond to the total mole equations for the species. As the solution is irradiated, the hydroxyl radicals are created and the oxidation process commences. During the reaction new species are created and others are consumed according to the reaction mechanism that has been presented. It is clear that such a process cannot be approximated using equilibrium models and that the kinetic approach is the correct way to model it.

Even though the reactions of the H_2O_2/UV oxidation process are very fast, equilibrium processes do take place and have to be considered. The species that have acid-base chemistry will develop nearly instantaneous equilibrium concentrations as the oxidation reactions progress. We have to formulate our model to resolve this equilibrium chemistry.

The model that has been developed considers the following reactions:

$$\begin{aligned}
&\frac{d[TOT_{H_2O_2}]}{dt} = RTOT_{H_2O_2} \\
&\frac{d[OH\bullet]}{dt} = R_{OH\bullet} \\
&\frac{d[TOT_{HO_2\bullet}]}{dt} = RTOT_{HO_2\bullet} \\
&\frac{d[CO_3^{-}\bullet]}{dt} = R_{CO_3^{-}\bullet} \\
&\frac{d[C_T]}{dt} = R_{C_T}
\end{aligned} \qquad (4.20)$$

and of course the phosphate esters reactions.

It is obvious that the above system of differential equations can be solved using infinitesimal time advancements; various efficient algorithms exist for such problems. After the end of each time step we have to consider the equilibrium concentrations for species that have acid-base chemistry. From the kinetic model the change in the total moles concentration has been calculated. At this point, the relevant mass laws have to be used to obtain the new instantaneous equilibrated concentrations of the weak acids and their conjugate bases.

A new step has to be introduced in our algorithm which results in the following equilibrium concentrations:

$$\begin{aligned}
&\frac{[HO_2^{-}][H^{+}]}{[H_2O_2]} = K_{H_2O_2} \\
&\frac{[O_2^{-}\bullet][H^{+}]}{[HO_2\bullet]} = K_{HO_2\bullet} \\
&\frac{[HCO_3^{-}][H^{+}]}{[H_2CO_3^{*}]} = K_{HCO_3^{-}} \\
&\frac{[CO_3^{-2}][H^{+}]}{[HCO_3^{-}]} = K_{CO_3^{-2}}
\end{aligned} \qquad (4.21)$$

The new equilibrated concentrations for the individual species can now be calculated from the total mole equation. At this step our algorithm assumes that pH is

constant through the reaction. This suggests that we assume a significant buffering capacity in our solution. This assumption is a simplifying one but not far fetched. In any case it is relatively straightforward to adjust the algorithm so that it calculates pH changes. Because the overall accuracy of the model presented here is limited by the lack of precise knowledge of some aspects of our system (for example: Unknown chemical composition of the treated water, simplified approach for the UV reactor), the addition of pH changes would be inappropriate. In a real-life design process, the exact chemistry of the treated water as well as the specifications of the UV reactor would be known. In such a case, introducing pH changes might be worthwhile.

Following our simplified approach, the exact concentration of hydrogen peroxide after each time step can be calculated as follows:

$$[HO_2^-] = K_{H_2O_2} \cdot [H_2O_2] \cdot [H^+]^{-1}$$
$$[H_2O_2] = \frac{TOT_{H_2O_2}}{(1+K_{H_2O_2}[H^+]^{-1})} \qquad (4.22)$$
$$[HO_2^-] = TOT_{H_2O_2} - [H_2O_2]$$

The same approach can be used for the other species with acid-base chemistry. The implementation of this approach within Matlab is described in section 4.4.

As we have seen when the mechanism of the AOP was developed, the overall reaction mechanism commences with the primary photolysis of hydrogen peroxide. It is obvious that this reaction is the one that governs the progress of the oxidation reaction. The rate with which the photolysis of hydrogen peroxide occurs can be derived based on the notion of quantum yield. Quantum yield is defined as:

$$\Phi_\lambda = \frac{\text{number of moles reacting}}{\text{number of einsteins absorbed}} \qquad (4.23)$$

The reaction rate then is equal to the quantum yield of hydrogen peroxide multiplied by the number of einsteins absorbed by hydrogen peroxide.

$$r_{UV,H_2O_2} = -\Phi_\lambda \cdot (\text{number of einsteins absorbed by } H_2O_2) \text{ [s-1]} \qquad (4.24)$$

The number of einsteins absorbed by hydrogen peroxide can be calculated using the point source summation method and Beer's law.

When the solution absorbs a small fraction of the energy of light, we can approximate Beer's law as a linear function of the intensity in the volume of solution that absorbs light and the properties of the solution. Since we are interested in the energy absorbed from hydrogen peroxide the expression becomes:

$$\text{Photons Absorbed per cm}^2 = 2.3 \cdot \varepsilon_{H_2O_2}(M^{-1}cm^{-1}) \cdot [H_2O_2] \cdot (M) \cdot \bar{I}(ein/cm^2) \cdot \text{pathlength (cm)}$$

For this to be true we need to apply this expression to very small volumes of the solution. The total absorbed energy from hydrogen peroxide will be the integral over the relevant volume.

The method was applied based on a numerical approach. Since the intensity of light is symmetrical regarding the angular coordinates in every cross section (at Zo), the calculations are done for 1 degree and then extended to the whole cross section. If we discretize the radius r in 1 cm lengths, we can calculate the intensity at every point using the point source summation method. The average intensity (eins) for the specified grid points is (points m and m+1):

$$\bar{I}_{m,m+1} = \frac{I(r_m, z_o) + I(r_{m+1}, z_o)}{2} \cdot \text{Area}_{m,m+1} \qquad (4.25)$$

where

$$\text{Area}_{m,m+1} = \frac{\frac{2\pi r_{m+1}}{360} + \frac{2\pi r_m}{360}}{2} \times 1 \text{ cm} \qquad (4.26)$$

so the absorbed energy for a one-degree width of the cross section is:

$$P_{1\text{ degree}} = 2.3 \cdot \varepsilon_{H_2O_2} \cdot [H_2O_2] \cdot \sum_{r_m=1}^{49} \frac{I(r_m, z_o) + I(r_{m+1}, z_o)}{2} \cdot \text{Area}_{m,m+1} \cdot (1 \text{ cm}) \quad (ein)$$

(4.27)

which can also be written as:

$$P_{1\ degree} = 2.3 \cdot \varepsilon_{H_2O_2} \cdot [H_2O_2] \cdot f(A)$$
$$f(A) = \sum_{r_m=1}^{49} \frac{I(r_m, z_o) + I(r_{m+1}, z_o)}{2} \cdot Area_{m,m+1} \cdot (1\ cm) \quad (ein) \tag{4.28}$$

The absorbed energy per unit volume of the cross section is:

$$PVolume_{1\ degree} = \frac{P_{1\ degree}\ (ein)}{\frac{(\pi \cdot 50^2 (cm^2) - \pi \cdot 1^2 (cm^2))}{360} \times 1\ cm} \ (ein/cm^3) \tag{4.29}$$

or

$$PVolume_{1\ degree} = \frac{2.3 \cdot \varepsilon_{H_2O_2} \cdot [H_2O_2] \cdot f(A)}{\frac{(\pi \cdot 50^2 (cm^2) - \pi \cdot 1^2 (cm^2))}{360} \times 1\ cm} \ (ein/cm^3) \tag{4.30}$$

and the average absorbed energy from hydrogen peroxide per volume in the reactor is:

$$PVolume_{Reactor} = \frac{\sum_{zo=1}^{zo=200} PVolume_{1\ degree}{}^{o}}{200} \ (ein/cm^3) \tag{4.31}$$

which can also be written as

$$PVolume_{Reactor} = [H_2O_2] \cdot \frac{2.3 \cdot \varepsilon_{H_2O_2}}{\frac{(\pi \cdot 50^2 - \pi \cdot 1^2)}{360}} \frac{\sum_{zo=1}^{zo=200} f(A)}{200} \ (ein/cm^3) \tag{4.32}$$

Since the intensity is a function of the absorbance of the solution and the absorbance is affected by the concentration of hydrogen peroxide, we can repeat the calculation steps and derive an expression for the average absorbed energy from hydrogen peroxide per volume in the reactor as a function of the hydrogen peroxide concentration. For this calculation, we assume a constant background absorbance of 0.02. The total absorbance of the solution is then given by

$$A = \left[[H_2O_2] \cdot \varepsilon_{H_2O_2} + [HO_2^-] \cdot \varepsilon_{HO_2^-} + \text{background absorbance} \right] (cm^{-1}) \tag{4.33}$$

For the range of pH encountered in natural waters the $\varepsilon_{HO_2^-}[HO_2^-]$ term can be neglected because the concentration of hydroperoxide ion is small (pKa of hydrogen peroxide is 11.6).

In what follows, the absorbed number of photons is given in einsteins per liter. The conversion from ein/cm^3 to ein/liter is straightforward (1000 cm^3 = 1 liter).

This procedure was done in Matlab and the results are:

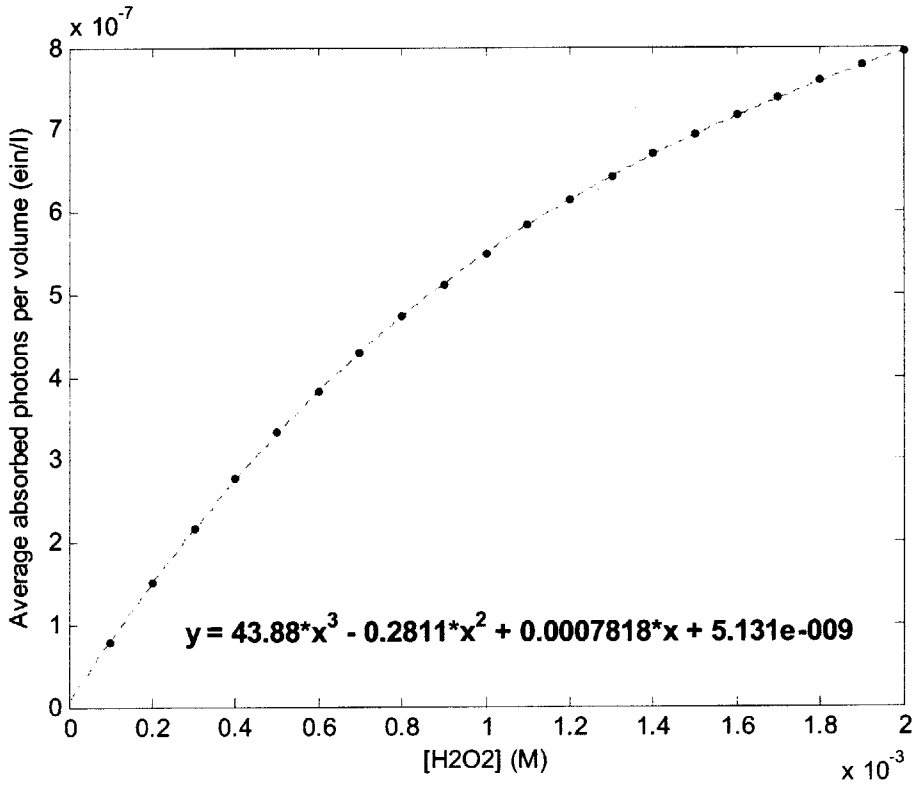

Figure 4-2 Average absorbed ein/liter per volume from hydrogen peroxide for a water with a background absorbance of water of 0.02 cm-1

From a curve fit of the above results, the average absorbed energy from hydrogen peroxide per volume in the reactor is given by the following expression:

$$\text{Absorbed}_{H_2O_2} = 43.88\cdot[H_2O_2]^3 - 0.2811\cdot[H_2O_2]^2 + 7.818\cdot10^{-4}\cdot[H_2O_2] + 5.131\cdot10^{-9} \quad \text{(ein/liter)}$$

(4.34)

We can also use the expression (4.32) which is a more general formulation and plot $\frac{2.3\cdot\varepsilon_{H_2O_2}}{(\pi\cdot50^2-\pi\cdot1^2)}\frac{\sum_{z=1}^{z=200} f(A)}{200}$ versus the total absorbance of the solution. This way for the given geometry of the reactor knowing the background absorbance and the hydrogen peroxide concentration we can calculate the absorbed energy from hydrogen peroxide per cross section.

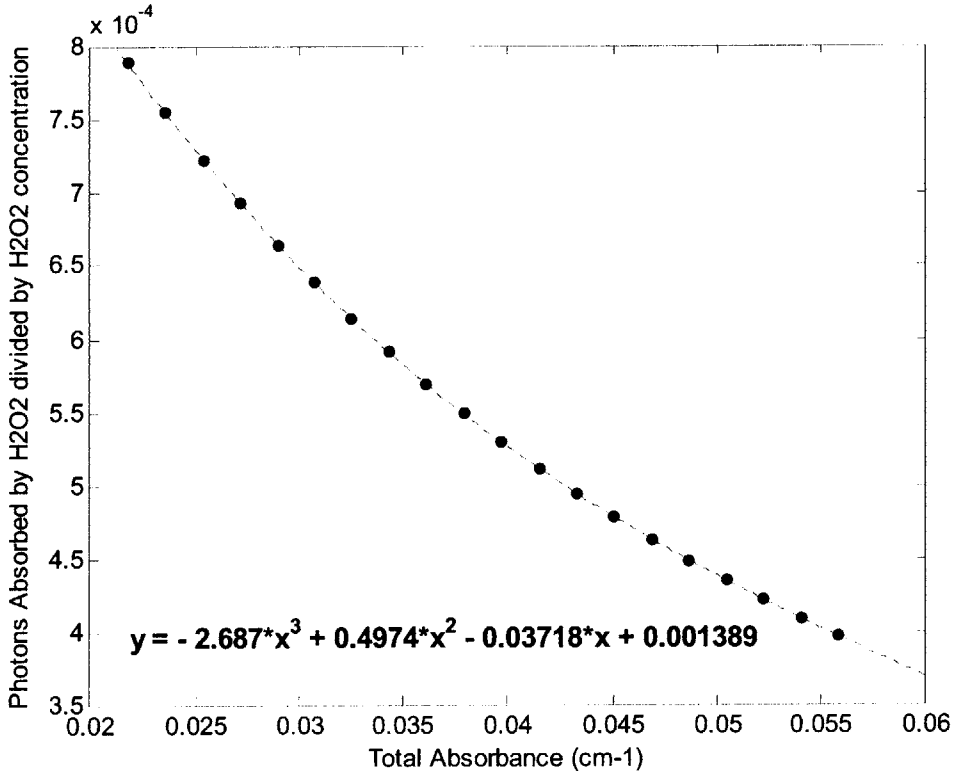

Figure 4-3 Average absorbed ein/liter per cross section from hydrogen peroxide divide by hydrogen peroxide concentration for a given range of total absorbance

With this formulation, we can compute the average absorbed photons by hydrogen peroxide in this reactor for any given total absorbance of the solution and hydrogen peroxide concentration.

$$\text{Absorbed}_{H_2O_2} = [H_2O_2] \cdot (-2.687 \cdot A^3 + 0.4974 \cdot A^2 - 0.03718 \cdot A + 0.001389) \quad \text{(ein/liter)} \tag{4.35}$$

When we designed the UV reactor we used a value of 0.02 cm^{-1} for the background absorbance of the solution which we will justify here. Whenever UV disinfection is used, special treatment processes are used to clarify water and decrease the concentrations of naturally occurring light absorbing species, but the water entering the UV reactor will still absorb some light. According to Masschelein (2002) the total absorbance at 254 nm of good quality distribution water (which is the goal at every drinking water treatment plant) is in the range of A ~ 0.02-0.11 cm^{-1}. Since special measures will be certainly taken to ensure the maximum effect of the UV irradiation, we assume that the water entering our reactor will have an absorbance in the lower bound of the range. This absorbance value is a lump sum parameter accounting for various naturally occurring species that absorb light. The most important are carbonate species, nitrate ion and dissolved organic matter. For quantitative reasons the absorbance of each of these species in a pure aqueous solution will be presented.

Table 4.3 Absorbance at 254 nm of significant constituents in natural waters. Data from: * Masschelein (2002) ** Voelker (1988), unpublished

Constituent	Absorbance (cm-1)
Nitrate ion (~ 0.8 mM) *	0.0025
Bicarbonate ion (~ 5mM) *	35*10-6
DOC (~ 0.4 mM) **	0.18
Per 0.01 mM DOC (Value expected for treated water)	0.0045

After the addition of hydrogen peroxide, the total absorbance of the solution will be:

$$A = \left[[H_2O_2] \cdot \varepsilon_{H_2O_2} + [HO_2^-] \cdot \varepsilon_{HO_2^-} + \text{other absorbing species} \right] (cm^{-1}) \qquad (4.36)$$

The extinction coefficient for hydrogen peroxide is 17.9 $M^{-1}cm^{-1}$ and 228 $M^{-1}cm^{-1}$ for HO_2^- respectively and for the term of background absorbance we assumed a value of 0.02 cm^{-1}.

At the end of every time step a new photolysis rate for hydrogen peroxide must be calculated based on the new concentrations that alter the absorbance of the solution.

One final consideration that must be taken into account has to do with the chemistry of the treated water. In the model up to now no other species that act as hydroxyl radical scavengers have been incorporated. One can choose to consider various different constituents of water; dissolved organic matter is very commonly considered. In the current model, it has been decided not to consider any other species besides the ones participating in the chain reaction (which include the carbonate species) and the phosphate esters.

This decision is based on the following two reasons. The exact chemistry of the water will be more accurately known in a real life design process. This will allow considering all the major constituents of the water in such a model using their exact concentration and their expected effect on the reaction. Therefore adding arbitrarily some tracer pollutants in our recipe to make the model more general increases the need for further assumptions and simplifications. That in turn compromises the accuracy of our model.

The other reason why such species will not be considered is the presence of hydrogen peroxide in our recipe. Hydrogen peroxide is a very effective hydroxyl radical scavenger (reported reaction rate constant is $2.7 \cdot 10^7$ $M^{-1}s^{-1}$, Buxton et al. 1988) and is present at a very high concentration during the AOP process. Unless some event causes tracer constituents that will survive the previous treatment stages to reach significant concentrations, hydrogen peroxide will be by orders of magnitude the most abundant hydroxyl radical scavenger present in our solution.

In the following, some issues that arise when programming the computer model have to be considered.

4.4 Issues about implementing the model in Matlab

The model was created in Matlab because the set of differential equations to be solved is very stiff. Any attempt to produce a home-made model in any generic programming language would create a problem relating to the choice of the time step. In the first few moments the gradients are so high that the time step has to be on the order of 10^{-10} sec. Special algorithms for the choice of an appropriate time step exist but the programming burden would be overwhelming compared to using Matlab's off-the-shelf solution.

Matlab comes with a suite of generic differential equation solvers that are optimized for different classes of problems. The "ode15s" solver, which is a variable order solver for stiff differential equations, was chosen here. The solver's performance is judged as excellent since it is very fast, robust and accurate. Special precautions were taken to increase the absolute tolerance of the solver to 10^{-20} due to the very small concentrations in some of the experiments.

Choosing an off-the-shelf package always creates some problems. In the case of Matlab, the main problem that had to be addressed is incorporating the mass laws in the solution procedure. As it has been mentioned before, the model is formulated in such a way as to give the overall rates for each family of species that exhibit acid base chemistry. This was done so that extending the model to consider pH changes would be straightforward and easy.

All the Matlab solvers are programmed to require the user to specify a differential rate of change for each one of the variables used in the system. This created the need to specify a rate of change for each individual species in the solution. To address this problem the rate of change of each individual species was associated with the total rate of change of the family of species with acid-base chemistry through the corresponding mass laws.

For example for the carbonate ions in the solution, the individual rates of change were obtained through the following manipulations

Since H_2CO_3* does not participate in the overall reactions and the pH of the solution is considered constant, the rate of change $r_{CO_3^{2-}/HCO_3^-}$ is equal to r_{Cl}. Using the mass laws we can now define the individual rates of change.

$$r_{HCO_3^-} = r_{C_T} \times \frac{[HCO_3^-]}{C_T} = \frac{r_{C_T}}{(1+10^{pH-10.33}+10^{6.35-pH})}$$

$$r_{CO_3^{-2}} = r_{C_T} \times \frac{[CO_3^{-2}]}{C_T} = \frac{r_{C_T}}{(1+10^{10.33-pH}+10^{16.68-2pH})} \qquad (4.37)$$

$$r_{H_2CO_3^*} = r_{C_T} \times \frac{[H_2CO_3^*]}{C_T} = \frac{r_{C_T}}{(1+10^{pH-6.35}+10^{2pH-16.68})}$$

This approach was used for all of the species that exhibit acid base chemistry.

5 Results of the model

The goal of this thesis is to explore the ability of the UV/H2O2 system to remove the phosphate esters from drinking water. It is clear that if such a process is necessary in the future, special design of the UV reactors will be used. In the current work, it has been assumed when developing the "ideal" UV reactor that design characteristics similar to the ones in water disinfection will be used. This poses a severe limitation since UV disinfection generally requires much lower exposure dosages than the oxidation of micro-pollutants through hydroxyl radical.

In the example runs of the model to follow, some of the properties of the solution will always be kept within a narrow range. This is because we are interested in applying such a treatment process to natural waters that are destined to reach distribution networks. The chemistry of good quality freshwater generally tends to be pretty consistent concerning the two major parameters that influence the performance of the UV/H2O2 process, pH and the total carbonate species.

The typical pH of natural waters is in the range of 6 to 9 and the typical concentration of total carbonate species (C_T) is in the range of 10^{-4} to $5*10^{-3}$ M

The third important parameter of the performance of the UV/H2O2 process is the initial concentration of added hydrogen peroxide. As will be shown later, increasing the hydrogen peroxide dose up to a point improves the removal of the phosphate esters. Because hydrogen peroxide is mildly toxic, we are interested in the final concentration of hydrogen peroxide at the outflow of the UV reactor. In this work we will adopt as the desired outflow concentration of hydrogen peroxide the maximum allowed level for drinking water in Germany which is 17 mg/l. According to Masschelein (2002), this value will soon be adopted from the European Union. This concentration when translated to molar concentration becomes $5*10^{-4}$ M.

As an introduction to the results that this process is capable of achieving, the following plot of the concentrations of the phosphate esters is presented. This run of the model had as input parameters:

Table 5.1

Characteristics of Run	
Lamp Power	459 W
pH	7
Hydrogen peroxide [M]	0.0005
Ct [M]	0.0005
Exposure time	20 sec

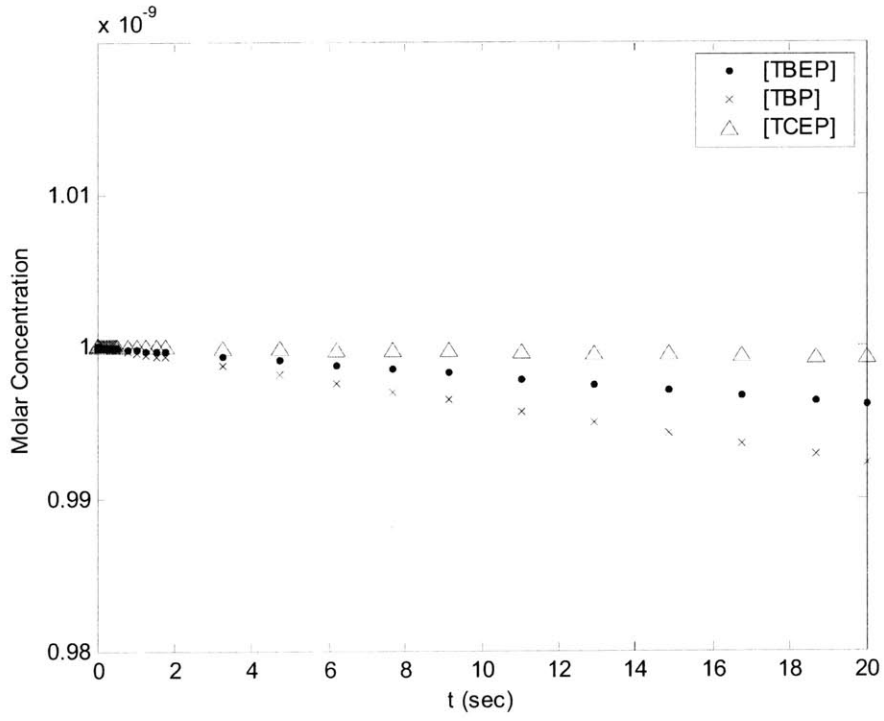

Figure 5-1 Degradation of phosphate esters. pH=7, C_T=0.0005 M and H_2O_2=0.0005 M

It is obvious that the efficiency of the process is very small for the given configuration. TBEP, which is the compound degrading the most, is removed at a percentage below 1%. It has to be noted that the hydrogen peroxide dose is exactly at the limit of $5*10^{-4}$ M.

The reaction mechanism as it was described earlier is very complicated and various radical ions are generated in the progress of the reaction. In the next plot, the concentration of some of these radicals for the same run is presented as it evolves in time.

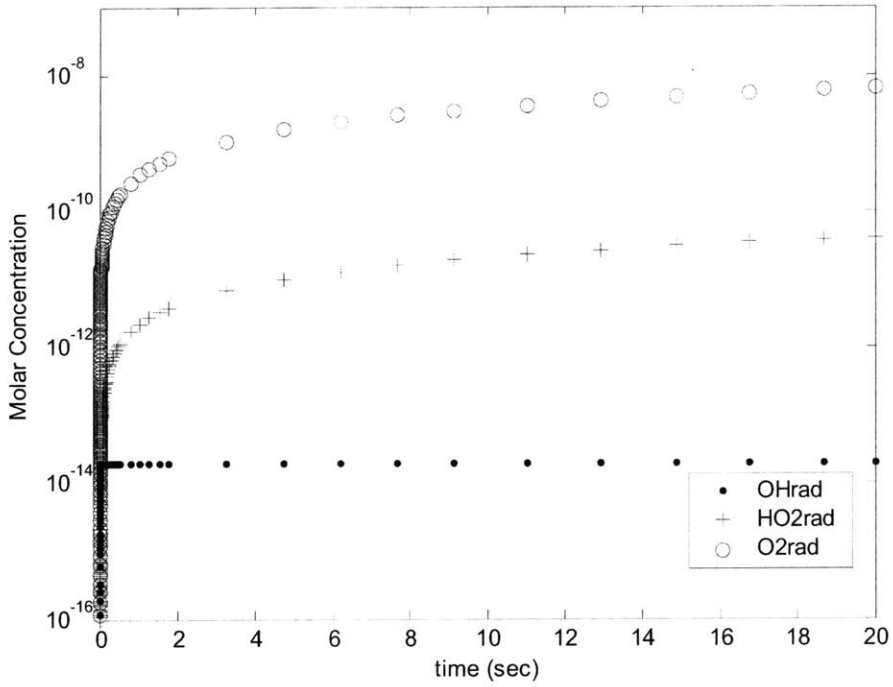

Figure 5-2 Radical Concentrations for the same run

From figure 5-2 we can see that the hydroxyl radical has the lowest steady state concentration of the radicals that are generated in the reaction. This happens because hydroxyl radical is the most reactive of all the radicals and is consumed almost instantaneously. We can also note that $HO_2\bullet$ concentration is significantly lower than $O_2^-\bullet$ concentration. This is expected since $HO_2\bullet$ is a weak acid with a pKa = 4.8 and in the pH of the run (pH=7) almost completely dissociates to $O_2^-\bullet$.

Before applying the model for specific real life conditions, we will explore how the chemistry of water affects the efficiency of the treatment process.

5.1 Solution recipe and efficiency of the process

In the following we will examine the effects of the chemistry of the solution and we will try to find the conditions optimizing the efficiency of the UV/H2O2 treatment process. The master variables for this treatment process are the pH of the solution, the concentration of carbonate species and the initial dose of hydrogen peroxide. All of these parameters influence the efficiency in different ways that are going to be examined in the following. Finally the effect of light intensity will be discussed.

An easy way to quantify the efficiency of the treatment process is by comparing the pseudo-first-order reaction rate coefficients of degradation of the phosphate esters. In the conditions simulated in this work, their degradation is almost linear with time so a pseudo first order reaction rate is a valid measure of the efficiency of the treatment process.

5.2 Effects of pH

Holding the total inorganic carbonate concentration and the initial hydrogen peroxide dose steady and changing the pH of the solution allows us to study the effects of pH on the efficiency of the solution. In the following figure, the pseudo-first-order rate coefficients are shown as a function of the solution pH. The first order decay rate coefficients were calculated as: $k_{TBP} = -\frac{\ln([TBP_{final}]/[TBP_{initial}])}{t}$

The parameters for the simulations are:

Table 5.2

Characteristics of Runs	
Lamp Power	459 W
pH	5 - 12
Hydrogen peroxide [M]	0.001
Ct [M]	0.001
Exposure time	20 sec

It is obvious that the increase in the pH of the solution decreases the pseudo-first-order rate coefficients. This is because increase in the pH affects the species that exhibit acid-base chemistry and alters their equilibrium concentrations.

The major hydroxyl radical scavengers in natural waters are the carbonate species. When the pH increases, the dissociation of bicarbonate ion to carbonate ion increases, rendering the carbonate species an even more effective scavenger

$$OH\bullet + CO_3^{2-} \rightarrow CO_3^{-}\bullet + OH^{-}, \qquad k_6 = 3.9\times10^{8} \quad (5.1)$$

$$OH\bullet + HCO_3^{-} \rightarrow CO_3^{-}\bullet + H_2O, \qquad k_7 = 8.5\times10^{6} \quad (5.2)$$

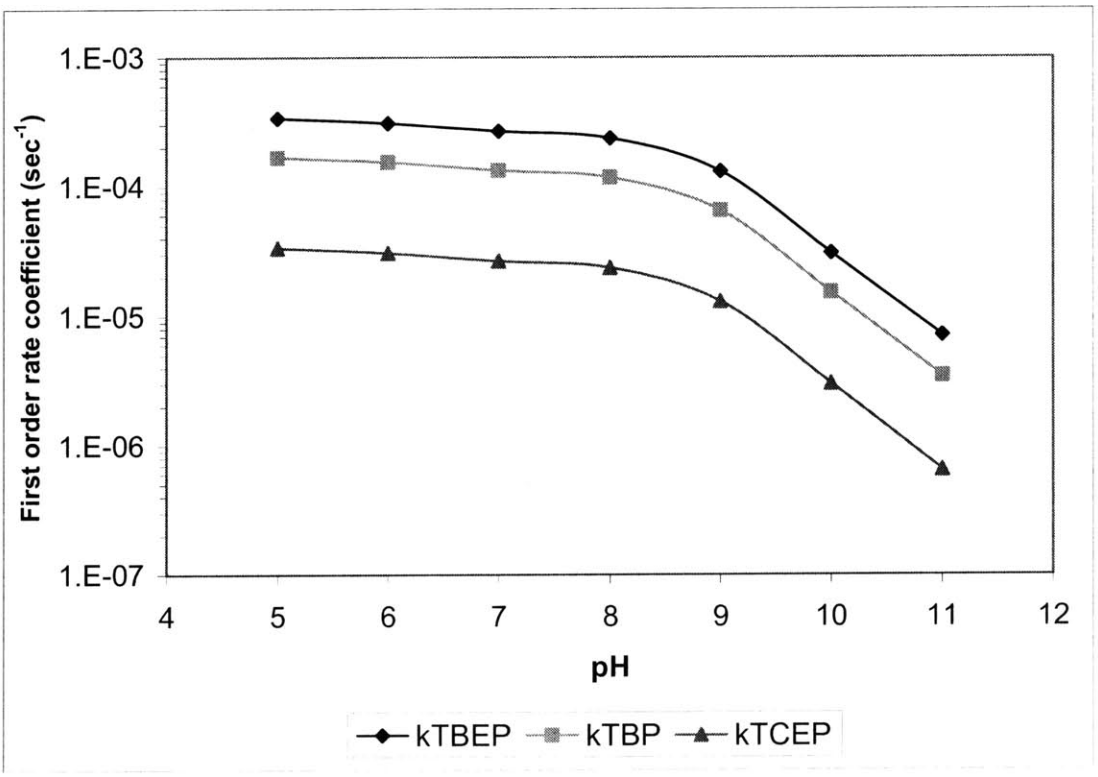

Figure 5-3 First order reaction rate coefficients vs. pH. $H_2O_2=10^{-3}$ M, $C_T=10^{-3}$ M

Another effect of increasing the pH is that the concentration of hydroperoxide ion increases from the dissociation of hydrogen peroxide. Again, hydroperoxide ion is a more effective hydroxyl radical scavenger and this affects the efficiency of the process.

$$H_2O_2 + OH\bullet \rightarrow H_2O + HO_2\bullet, \qquad k_2 = 2.7\times10^7 \quad (5.3)$$

$$OH\bullet + HO_2^- \rightarrow HO_2\bullet + OH^-, \qquad k_3 = 7.5\times10^9 \quad (5.4)$$

From figure 5-3 it is obvious that when the pH is low, an increase does not affect the pseudo-first-order rates significantly. From pH 8 and above, any increase in the pH has dramatic effects in the efficiency of the process. This can be explained based on the pKa values of the carbonate species and hydrogen peroxide.

$$H_2CO_3^* \rightleftharpoons H^+ + HCO_3^-, \qquad pK_{a1} = 6.35 \quad (5.5)$$

$$HCO_3^- \rightleftharpoons H^+ + CO_3^{2-}, \qquad pK_{a2} = 10.33 \quad (5.6)$$

$$H_2O_2 \rightleftharpoons H^+ + HO_2^-, \qquad pK_{a5} = 11.6 \quad (5.7)$$

For low pH values (<6) most of the inorganic carbonate is present as $H_2CO_3^*$ which does not take part in the reaction mechanism. For pH values above pH=8 the carbonate ion starts having a significant concentration and reduces the efficiency of the process. At really high pH values (abnormal for natural waters) most of the carbonate species are present as carbonate ion and significant percentage of hydrogen peroxide is dissociated to hydroperoxide ion, rendering the solution an excellent hydroxyl radical scavenger.

Since natural waters typically have a pH in the range of 6 to 9 it is not expected that pH will pose a significant problem for the efficiency of the process. In any case, artificial lowering of the pH is advantageous for the process.

5.3 Effects of C_T

The effect of the concentration of carbonate species is easily predictable. Increasing their concentration decreases the pseudo-first-order rate coefficients because the scavenging of hydroxyl radical is increased. A series of simulations were done to show this effect.

Table 5.3

Characteristics of Runs	
Lamp Power	459 W
pH	8
Hydrogen peroxide [M]	0.001
Ct [M]	1*10^-4 - 7.5*10^-3
Exposure time	20 sec

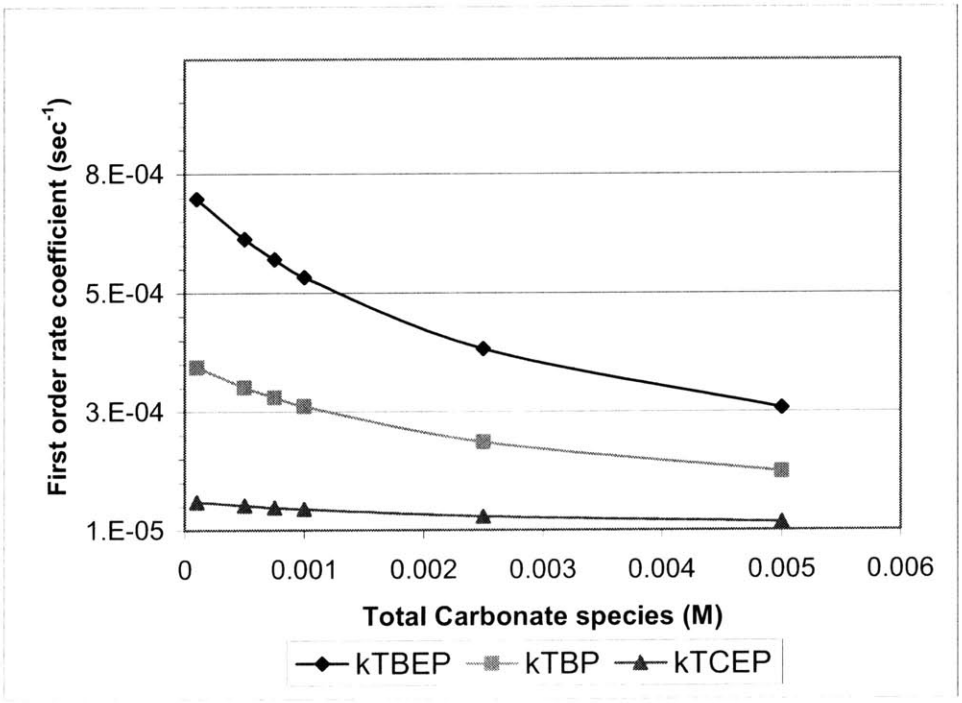

Figure 5-4 First order reaction rate coefficients vs. C_T. $H_2O_2=10^{-3}$ M, pH=8

Decreasing the concentration of carbonate species significantly improves the efficiency of the process. Therefore pre-softening of high alkalinity waters is suggested

5.4 Effects of initial Hydrogen Peroxide dose

The hydrogen peroxide dose is a very important parameter for the efficiency of the treatment process and the economic desirability. In the UV/H2O2 process, the photolysis of hydrogen peroxide is the major mechanism generating hydroxyl radicals. Therefore it is logical to assume that increasing the dose of hydrogen peroxide would increase the steady-state concentration of hydroxyl radicals. This is not the case though, because hydrogen peroxide acts as a hydroxyl radical scavenger too.

$$H_2O_2/HO_2^- + OH\bullet \rightarrow H_2O/OH^- + HO_2 \quad (5.8)$$

with a reaction rate constant $k_2 = 2.7 \times 10^7\ M^{-1}s^{-1}$ for hydrogen peroxide and $k_3 = 7.5 \times 10^9$ for hydroperoxide ion.

In order to show the effect of the initial H_2O_2 concentration on the pseudo-first-order rate constants of the phosphate esters a series of simulations were done with increasing the hydrogen peroxide dose. The input parameters were:

Table 5.4

Characteristics of Runs	
Lamp Power	459 W
pH	7
Hydrogen peroxide [M]	5*10^-5 - 10^-2
Ct [M]	0.001
Exposure time	20 sec

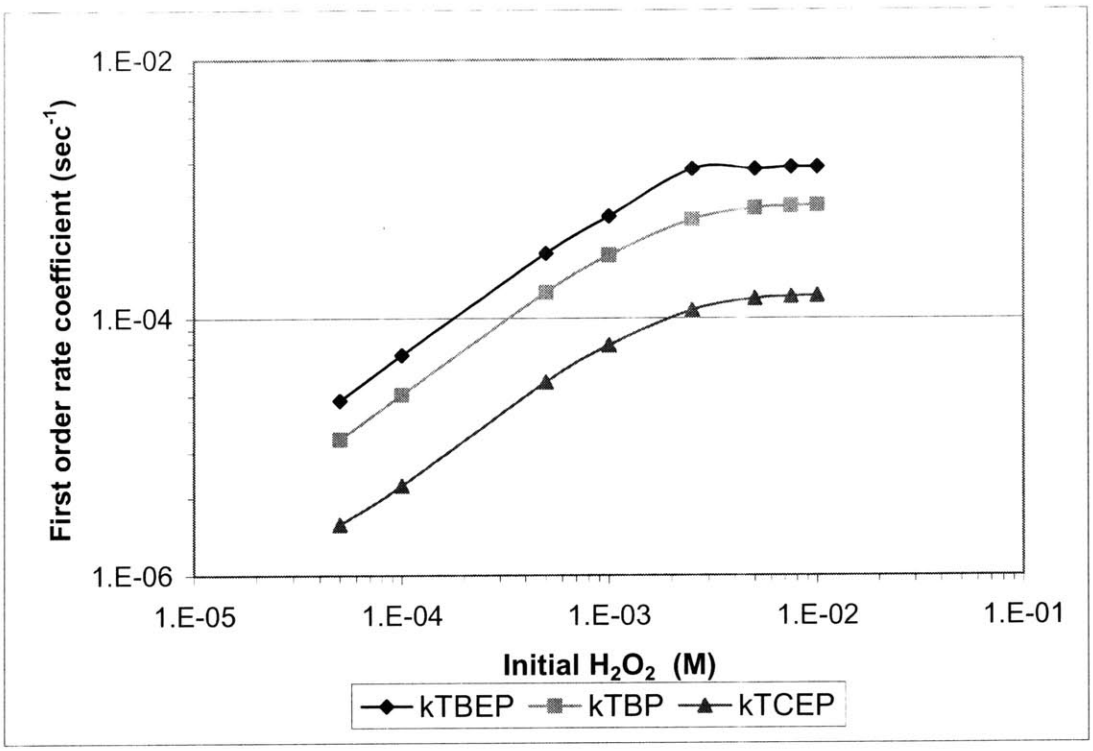

Figure 5-5 First order reaction rate coefficients vs. H_2O_2. = C_T =10^{-3} M, pH=7

From figure 3, it is obvious that at low initial hydrogen peroxide concentrations, increasing the dose significantly increases the degradation rate of the phosphate esters. At higher concentrations (>0.005 M), the effect of increasing the dose is negligible.

Glaze, Lay & Kang (1995) report that in the experiments they conducted on degradation of DBCP, the pseudo-first-order rate coefficient exhibited a maximum value when increasing the H_2O_2 dose and then declined. This is a reasonable result since the hydroxyl radical production is limited from the photolysis rate (when hydrogen peroxide absorbs all the available light). Increasing the hydrogen peroxide dose further from that point acts only to increase the hydroxyl radical scavenging from hydrogen peroxide. The model developed here does not predict such a behavior but that might be because the hydrogen peroxide doses implemented are not sufficiently high.

Since hydroperoxide ion is a more efficient hydroxyl radical scavenger than hydrogen peroxide, the change in the pseudo-first-order rate coefficients with increasing

concentration of hydrogen peroxide was compared for two different values of pH. For these simulations the carbonate species were neglected, so that only the effects of the hydrogen peroxide dissociation would be important. The simulations had the following characteristics:

Table 5.5

Characteristics of Runs	
Lamp Power	459 W
pH	7, 10
Hydrogen peroxide [M]	5*10^-4 - 10^-1
Ct [M]	0
Exposure time	20 sec

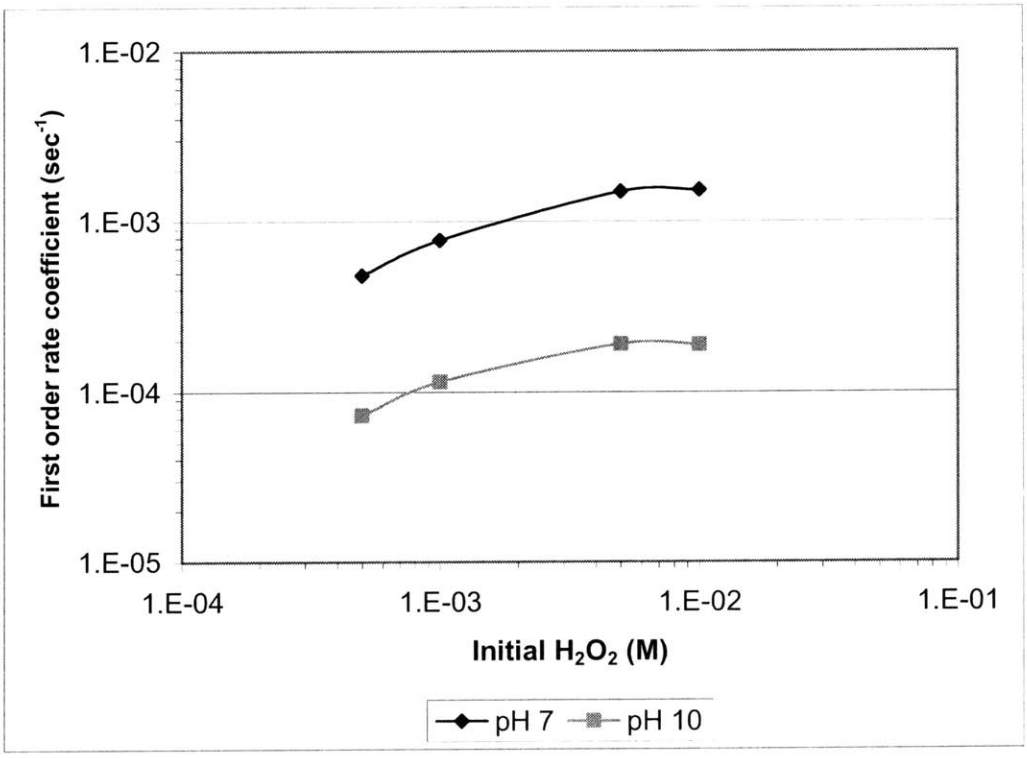

Figure 5-6 Effects of initial concentration of hydrogen peroxide for different values of pH on the pseudo-first-order rate coefficient for TBEP

We can observe that in absence of carbonate species the effect of increasing the hydrogen peroxide dose in different pH values is just a vertical displacement.

5.5 Effects of Lamp power

The effect of the lamp power is expected to be straightforward. Since the major mechanism for generation of hydroxyl radical is photolysis of hydrogen peroxide, increasing the power of the UV lamp should increase the generation rate of hydroxyl radical and thus the oxidation of the phosphate esters. For the following simulations, an increased light power was assumed (by a factor of 5, 10 and 50). Since the absorbed photons per volume are proportional to the lamp power, the original expression for the average absorbed energy from hydrogen peroxide per volume in the reactor can be used multiplied by the relevant factor

The following simulations were done:

Table 5.6

Characteristics of Runs	
Lamp power	1,5,10,50* 459 W
pH	8
Hydrogen peroxide [M]	0.005
Ct [M]	0.0005
Exposure time	20 sec

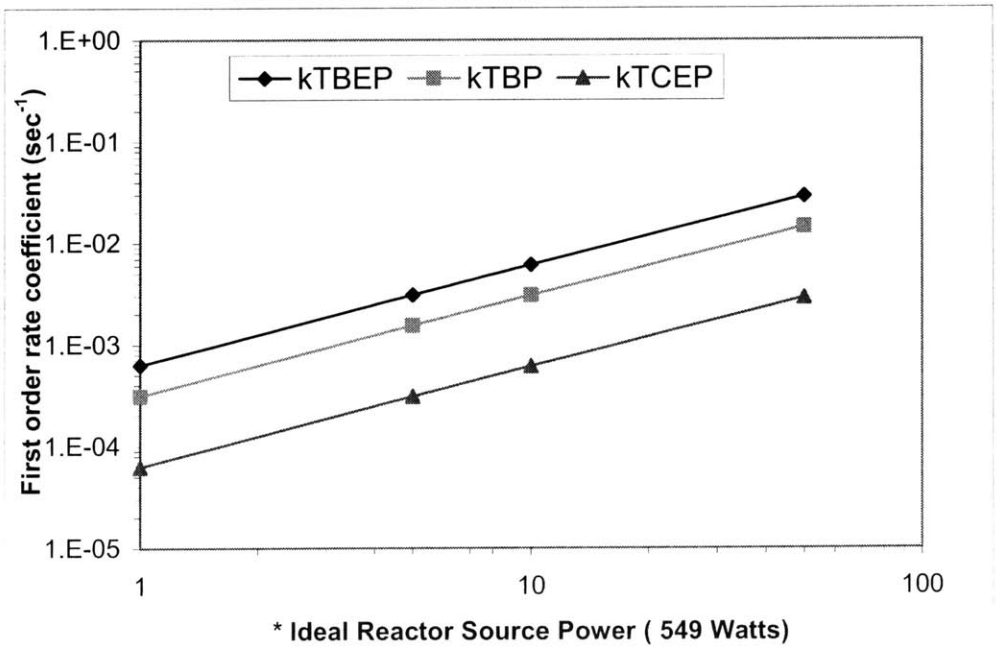

Figure 5-7 First order reaction rate coefficients vs. lamp power. $H_2O_2=10^{-3}$ M, pH=8, $C_T=5*10^{-4}$ M

5.6 Steady state considerations and quick and dirty calculations

When the micro-pollutants exist in very small concentrations and the pH of the solution does not change significantly, the hydroxyl radical concentration reaches a steady state. For the preliminary design steps, a steady-state assumption can be used to provide the basic required characteristics of the UV reactor and the recipe of the solution.

Assuming a steady-state concentration of hydroxyl radical and a known initial concentration of a micro-pollutant, we can predict the latter's removal rate in the UV reactor. For example for TBP we would have:

$$\frac{\mathrm{dTBP}}{\mathrm{dt}} = -k_{\mathrm{TBP}} \cdot [\mathrm{OH}\bullet]_{\mathrm{SS}} \cdot [\mathrm{TBP}] \qquad (5.9)$$

$$[\mathrm{TBP}]_{\mathrm{final}} = [\mathrm{TBP}]_{\mathrm{o}} \cdot e^{-k_{\mathrm{TBP}} \cdot [\mathrm{OH}\bullet]_{\mathrm{SS}} \cdot t} \qquad (5.10)$$

so constant $[OH\bullet]_{SS}$ leads directly to a pseudo-first-order rate coefficient.

It is evident that formulating an expression for pseudo-steady-state concentration of hydroxyl radical is very helpful. The first step is to assume that the rate of change of hydroxyl radical is zero, and by an order of magnitude analysis to neglect some of the terms.

$$\begin{aligned} r_{OH\cdot} = 0 = {} & 2 \cdot r_{UV,OH\cdot}[H_2O_2] - k_2[H_2O_2][OH\bullet] - k_3[HO_2^-][OH\bullet] \\ & + k_4[H_2O_2][HO_2\bullet] + k_5[H_2O_2][O_2^-\bullet] \\ & - k_6[OH\bullet][CO_3^{2-}] - k_7[OH\bullet][HCO_3^-] \\ & - k_{10}[OH\bullet][OH\bullet] - k_{11}[OH\bullet][HO_2\bullet] \\ & - k_{14}[OH\bullet][O_2^-\bullet] - k_{15}[OH\bullet][CO_3^-\bullet] \\ & - k_{TBP}[OH\bullet][TBP] - k_{TCEP}[OH\bullet][TCEP] - k_{TBEP}[OH\bullet][TBEP] \end{aligned} \qquad (5.11)$$

This expression can be re-arranged to give the steady-state concentration of hydroxyl radicals. Because $k_{10}[OH\bullet][OH\bullet]$ is too small it has been neglected.

$$[OH\bullet]_{SS} = \frac{2 \cdot r_{UV,OH\bullet}[H_2O_2] + k_4[H_2O_2][HO_2\bullet] + k_5[H_2O_2][O_2^-\bullet]}{k_2[H_2O_2] + k_3[HO_2^-] + k_6[CO_3^{2-}] + k_7[HCO_3^-] + k_{11}[HO_2\bullet] \ldots} \quad (5.12)$$
$$\ldots + k_{14}[O_2^-\bullet] + k_{15}[CO_3^-\bullet] + k_{TBP}[TBP] + k_{TCEP}[TCEP] + k_{TBEP}[TBEP]$$

For typical values of pH, C_T and initial H_2O_2 dose such as pH=7, $C_T=5*10^{-4}$ M and initial $H_2O_2=10^{-3}$ M we have:

$$\begin{aligned} &H_2O_2 \sim 10^{-3} \\ &HO_2\bullet \sim 10^{-9} \\ &O_2^-\bullet \sim 10^{-7} \end{aligned} \quad (5.13)$$

and the order of magnitude of the various parameters is:

$$\begin{aligned} &k_2[H_2O_2] \sim 10^4 \text{ important} \\ &k_3[HO_2^-] \sim 10^3 \text{ important} \\ &k_4[H_2O_2][HO_2\bullet] \sim 10^{-13} \text{ neglected} \\ &k_5[H_2O_2][O_2^-\bullet] \sim 10^{-11} \text{ neglected} \\ &k_6[CO_3^{2-}] \sim 10^3 \text{ important} \\ &k_7[HCO_3^-] \sim 10^3 \text{ important} \\ &k_{11}[HO_2\bullet] \sim 10^{-2} \text{ neglected} \\ &k_{14}[O_2^-\bullet] \sim 10^2 \text{ neglected} \\ &k_{15}[CO_3^-\bullet] \sim 10^{-2} \text{ neglected} \\ &k_{TBP}[TBP] \sim 1 \text{ neglected} \\ &k_{TCEP}[TCEP] \sim 1 \text{ neglected} \\ &k_{TBEP}[TBEP] \sim 1 \text{ neglected} \end{aligned} \quad (5.14)$$

These approximations lead to the following expression for the steady-state concentration of hydroxyl radicals:

$$[OH\bullet]_{SS} = \frac{2 \cdot r_{UV,OH\bullet}[H_2O_2]}{k_2[H_2O_2] + k_3[HO_2^-] + k_6[CO_3^{2-}] + k_7[HCO_3^-]} \quad (5.15)$$

For a given recipe of the solution (pH, C_T and initial H_2O_2 dose) the expression can be evaluated.

A series of simulations were conducted to estimate the error introduced by using the previous expression to evaluate the steady-state concentration of hydroxyl radical.

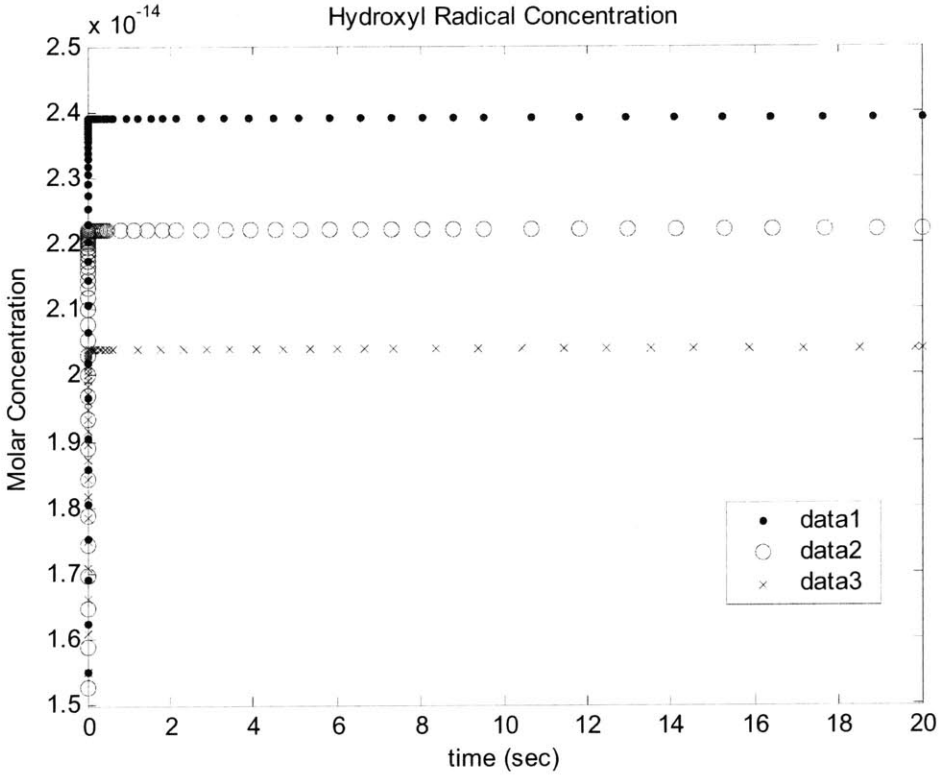

Figure 5-8 Selected runs, it is obvious that a steady state situation is reached

In table 5.7 the results of the simulations are presented. The error is calculated as:

$$error = \left| \frac{simulated - predicted}{simulated} \right| \% \qquad (5.16)$$

Table 5.7 **Pseudo steady state assumption, Results**

	pH	Ct	H2O2o	Predicted	Simulated	Error
1	6	0.0001	0.0005	2.4E-14	2.4E-14	0.11%
2	6	0.0005	0.0005	2.2E-14	2.2E-14	0.09%
3	6	0.001	0.0005	2.0E-14	2.0E-14	0.06%
4	7	0.0001	0.0005	2.3E-14	2.3E-14	0.25%
5	7	0.0005	0.0005	1.9E-14	1.9E-14	0.19%
6	7	0.001	0.0005	1.6E-14	1.6E-14	0.13%
7	8	0.0001	0.0005	2.1E-14	2.1E-14	0.27%
8	8	0.0005	0.0005	1.7E-14	1.7E-14	0.19%
9	8	0.001	0.0005	1.3E-14	1.3E-14	0.13%
10	9	0.0001	0.0005	1.3E-14	1.3E-14	0.35%
11	9	0.0005	0.0005	9.4E-15	9.4E-15	0.29%
12	9	0.001	0.0005	7.0E-15	6.9E-15	0.25%

From table 5.7 we can see that the steady-state assumption gives very accurate results. Of course such a simplifying approach needs to be used with caution, but for preliminary design calculations it could give useful insight.

Under certain conditions the steady-state assumption made by equation (5.15) can be invalid. Equation (5.15) considers scavenging of hydroxyl radicals only from hydrogen peroxide and carbonate species. This is consisted with the typically encountered concentrations of the other scavenging species in natural waters but leads to significant errors if their concentrations are greatly increased in the solution.

For example if in the solution, the phosphate esters are present at high concentrations (order of 10^{-4} to 10^{-6} M) and the irradiation dose is greatly increased the situation is unsteady and the simplifying assumptions cannot be made. In the following figure such a case is presented, and it is clear that predicting the reaction rates would be more complicated.

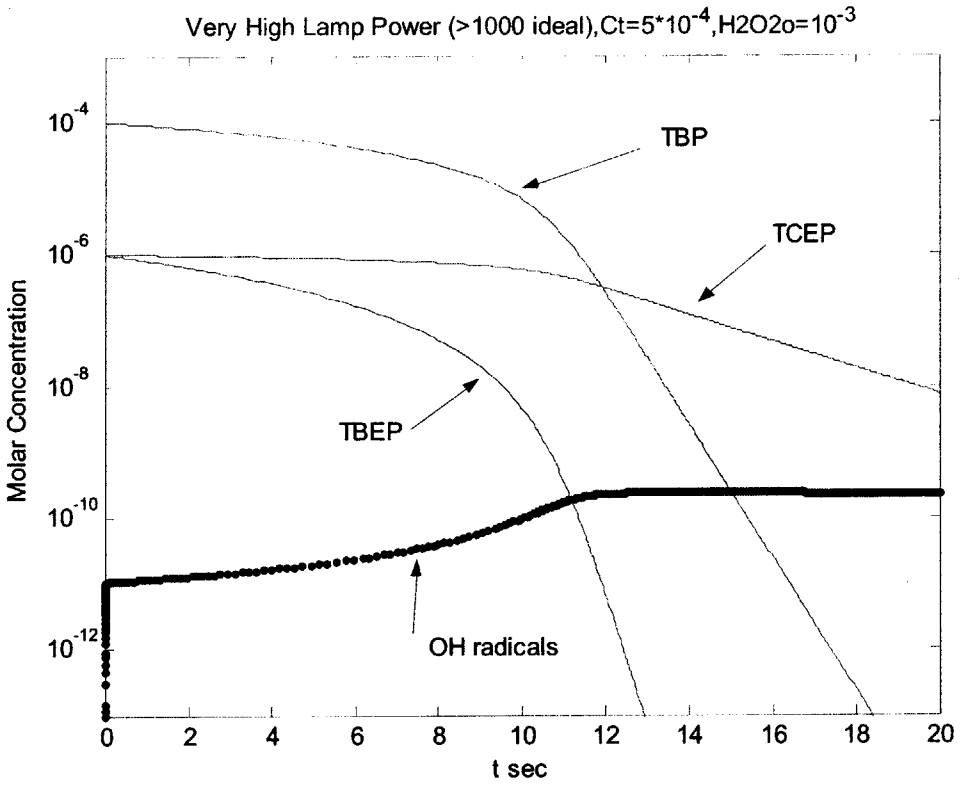

Figure 5-9 A very unsteady case

From Figure 5-9 we can observe that the hydroxyl radical concentration increases significantly between time zero and t =12 sec where a steady state concentration is reached. This is due to the significant presence of the phosphate esters which are very efficient hydroxyl radical scavengers. Initially, the phosphate esters are present at such concentrations that their scavenging effect is comparable to or greater than the one from the hydrogen peroxide and carbonate species. As they degrade, their relevant effect is diminished and for t=12 and above their effect becomes negligible compared to the scavenging species considered in equation (5.15).

The expression for the steady state concentration of hydroxyl radical can be used to validate our observations on the various parameters that affect the pseudo-first-order reaction rate coefficients of the phosphate esters.

$$[\mathrm{OH}\bullet]_{SS} = \frac{2 \cdot r_{UV,OH\bullet}[H_2O_2]}{k_2[H_2O_2] + k_3[HO_2^-] + k_6[CO_3^{2-}] + k_7[HCO_3^-]} \qquad (5.17)$$

It is obvious that any increase in the total carbonate species in our recipe decreases the steady state concentration of hydroxyl radicals and therefore slows down the oxidation process. Increasing the UV light intensity increases the numerator of the expression and thus increases the concentration of hydroxyl radicals.

The effect of pH on the steady state concentration of hydroxyl radical is more interesting. The values for the rate constants are:

$$k_2 = 2.7 \times 10^7 \ M^{-1}s^{-1} \qquad (5.18)$$

$$k_3 = 7.5 \times 10^9 \ M^{-1}s^{-1} \qquad (5.19)$$

$$k_6 = 3.9 \times 10^8 \ M^{-1}s^{-1} \qquad (5.20)$$

$$k_7 = 8.5 \times 10^6 \ M^{-1}s^{-1} \qquad (5.21)$$

and the acid base related dissociation constants are

$$H_2O_2 \rightleftharpoons H^+ + HO_2^-, \qquad pK_{a5} = 11.6 \qquad (5.22)$$

$$HCO_3^- \rightleftharpoons H^+ + CO_3^{2-}, \qquad pK_{a2} = 10.33 \qquad (5.23)$$

$$H_2CO_3^* \rightleftharpoons H^+ + HCO_3^-, \qquad pK_{a1} = 6.35 \qquad (5.24)$$

From the rate constants and the dissociation constants is clear than increasing pH decreases the steady state hydroxyl radical concentration. What is more interesting is to find an explanation for the dramatic decrease in the first order reaction rate coefficients of the phosphates when pH is above pH = 8.

Substituting the rate constant and using the mass laws we can write the expression for the steady state concentration of hydroxyl radicals as a function of total hydrogen peroxide species, total carbonate species and pH.

$$[OH\bullet]_{SS} = \frac{2 \cdot r_{UV,OH\bullet} \cdot \frac{H_2O_{2\,T}}{1+10^{pH-11.6}}}{H_2O_{2\,T} \cdot \left(2.7 \cdot 10^7 \cdot \frac{1}{1+10^{pH-11.6}} + 7.5 \cdot 10^9 \cdot \frac{1}{1+10^{11.6-pH}}\right) + \\ + C_T \cdot \left(3.9 \cdot 10^8 \cdot \frac{1}{1+10^{10.33-pH}+10^{16.68-2pH}} + 8.5 \cdot 10^6 \cdot \frac{1}{1+10^{pH-10.33}+10^{6.35-pH}}\right)}$$

(5.25)

The expressions can now be evaluated for any value of pH if we substitute the values for total hydrogen peroxide species, total carbonate species and the photolysis rate. Using typical values for C_T and $H_2O_{2\,T}$ of 0.0005 M and calculating the photolysis rate with equation (5.25) the following plot was created.

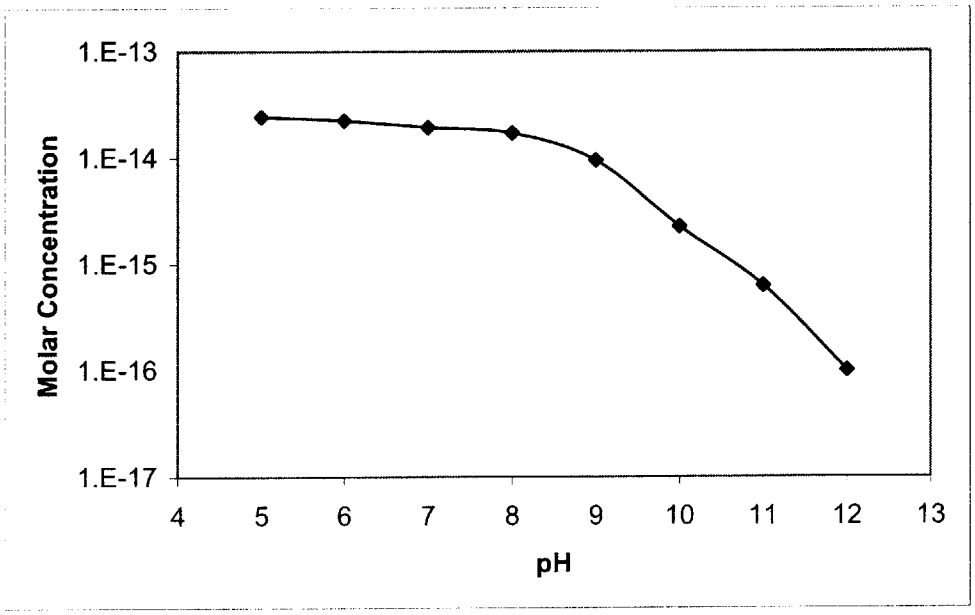

Figure 5-10 Steady state concentration of hydroxyl radicals vs. pH. Ct = 0.0005 M and H2O2 total =0.0005 M

We can observe from figure 5-10 that the steady-state concentration of hydroxyl radicals declines very fast for pH values above 8. This explains clearly the dramatic decrease in the first order reaction rate coefficients of the phosphates when pH is above pH = 8.

Equation (5.25) predicts that the pH where the steady-state concentration of hydroxyl radical with regard to pH changes declines very fast is a function of the ratio of the concentration of hydrogen peroxide species to carbonate species. Figure 5-11 shows the effect of varying the $\frac{[H_2O_2]_T}{C_T}$ ratio.

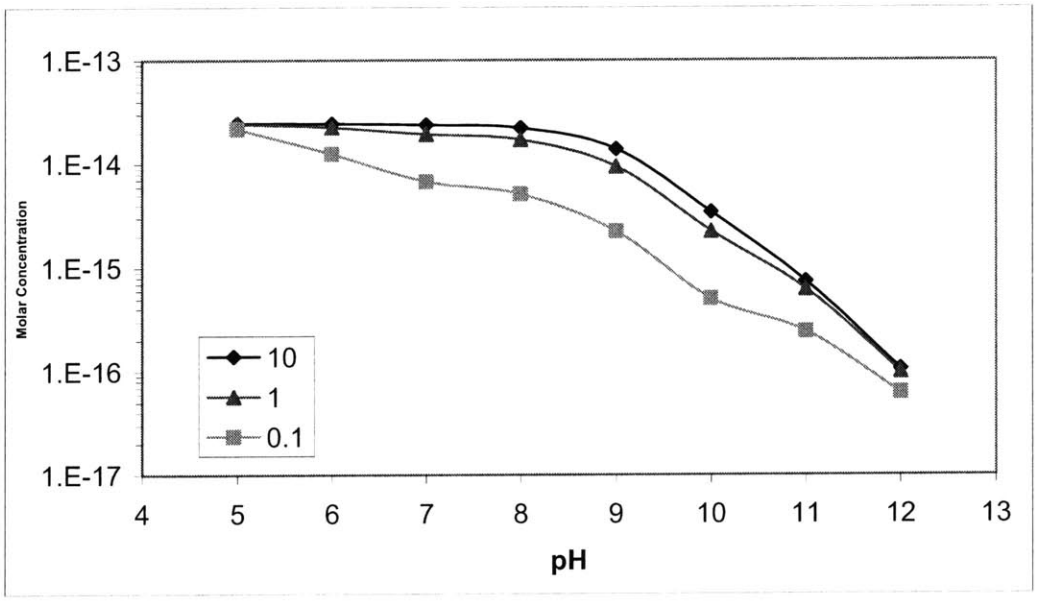

Figure 5-11 Steady state concentration of hydroxyl radicals vs. pH. For ratios of $\frac{[H_2O_2]_T}{C_T}$ = 10, 1 and 0.1

When the ratio of $\frac{[H_2O_2]_T}{C_T}$ is high (10) the decline of the steady state concentration of hydroxyl radicals is governed by the dissociation of hydrogen peroxide to hydroperoxide ion. Since the pKa is11.6 and the relevant scavenging rates differ by a

factor of ~300 the effect of the dissociation becomes significant around pH= 9. In contrast when the ration of $\frac{[H_2O_2]_T}{C_T}$ is low (0.1) the decline of the steady state concentration of hydroxyl radicals is governed by the double dissociation of the carbonate species. The pKa's are 6.35 and 10.33 and around these pH values we can observe a sharp decline of the hydroxyl radical steady state concentration.

5.7 Atlanta Water Works

Lin (2004) conducted a study on the fate of flame retardants in the Atlanta Water Works drinking water treatment plant in Atlanta, Georgia and reports values for the phosphate esters concentration after the filtration step.

Table 5.8 **From Lin (2004)**

Pollutant	ug/l	[M]
TBP	0.019	7.0E-11
TBEP	0.444	1.6E-09
TCEP	0.158	4.0E-10

In addition, Lin reports values for the pH at the various treatments stages. After filtration the pH is 6.6. Unfortunately the C_T is not reported for the sampled water but pre-softening treatment of the water is done.

Using the values from table 5.8 the reported pH value and reasonable values for C_T, we will estimate the potential removal that the UV/H2O2 process could accomplish.

It has been assumed that since pre-softening of the water is used the total carbonate species can be as low as 10^{-4} M.

From table 5.9 it is obvious that when the "ideal" reactor is used that has been designed based only on disinfection requirements there is very small removal of the phosphate esters.

In table 5.10 the same simulations are presented but this time the UV light source power in the reactor is increased by a factor of 10 and a factor of 50.

Table 5.9 **Base case removal**

Lamp power	459 W
Ct	10^-4
pH	6.6

	Initial	Final	Removal	1st order
H2O2	5.0E-04			
TBP	7.0E-11	7.0E-11	0.5%	2.3E-04
TCEP	4.0E-10	4.0E-10	0.1%	4.6E-05
TBEP	1.6E-09	1.6E-09	0.9%	4.7E-04

When the intensity is increased by a factor of 50 the removal efficiency of the treatment process becomes significant. TBEP is removed at a ~36% level and TBP at level of ~20%. TCEP is removed at a lower level, ~5%, due to the slower reaction rate constant.

Table 5.10 **Increase in the UV lamp power**

Lamp power	10* 459W
Ct	10^-4
pH	6.6

	Initial	Final	Removal	1st order
H2O2	5.0E-04			
TBP	7.0E-11	6.7E-11	4.5%	2.3E-03
TCEP	4.0E-10	4.0E-10	0.9%	4.6E-04
TBEP	1.6E-09	1.5E-09	8.8%	4.6E-03

Lamp power	50* 459W
Ct	10^-4
pH	6.6

	Initial	Final	Removal	1st order
H2O2	5.0E-04			
TBP	7.0E-11	5.6E-11	20.1%	1.1E-02
TCEP	4.0E-10	3.8E-10	4.4%	2.2E-03
TBEP	1.6E-09	1.0E-09	36.2%	2.2E-02

In table 5.11 it has been assumed that there are three identical reactors in line. The UV lamp power is now 10 times the one used in the ideal reactor.

Table 5.11 **Three reactors in line**

Lamp power	10* 459 W
Ct	10^-4
pH	6.6

	Initial	Final	Removal	1st order
H2O2	5.0E-04			
TBP	7.0E-11	6.1E-11	12.9%	6.9E-03
TCEP	4.0E-10	3.9E-10	2.7%	1.4E-03
TBEP	1.6E-09	1.2E-09	24.1%	1.4E-02

The removal efficiency now reaches ~25% for TBEP, ~13% for TBP and ~3% for TCEP.

It is important to note that in the previous cases the dose of hydrogen peroxide complies with the limit of 17 mg/l mentioned before.

As a final scenario, we will consider the removal efficiency of 3 identical reactors in line with a UV lamp power 10 times the one used in the ideal reactor and a hydrogen peroxide dose of 10^{-3} M. This scenario is meant to resemble a design specifically targeted for the oxidation of micro-pollutants. The reason why here it was chosen to increase the hydrogen peroxide dose instead of increasing the UV lamp power is that it is less costly to increase the hydrogen peroxide dose and treat the water for the excess hydrogen peroxide than to increase the power of the UV lamp.

Table 5.12 Three reactors in line, Initial hydrogen peroxide 10^{-3} M

Lamp power	10* 459 W
Ct	10^-4
pH	6.6

	Initial	Final	Removal	1st order
H2O2	1.0E-03			
TBP	7.0E-11	5.6E-11	20.2%	1.1E-02
TCEP	4.0E-10	3.8E-10	4.4%	2.3E-03
TBEP	1.6E-09	1.0E-09	36.3%	2.3E-02

The removal efficiency now reaches ~36% for TBEP, ~20% for TBP and ~5% for TCEP. The magnitude of the removal is equal to the scenario of one reactor with 50 times the lamp power of the ideal reactor and a dose of hydrogen peroxide of $5*10^{-4}$ M. The removal in these two scenarios is significant and such a treatment process would offer a valid solution for the Atlanta Water Works plant if the removal of the phosphate esters from drinking water became a necessity.

6 Conclusions

In this work the issue removing phosphate esters from drinking water has been examined. From the various treatment processes available, the oxidation of phosphate esters through hydroxyl radical generated by the UV/H2O2 process was selected.

The results of the advanced oxidation process when applied in a UV unit specifically designed for disinfection purposes are not very encouraging. The potential removal of the phosphate esters under the UV intensity conditions specified by disinfection guidelines is very low.

From the analysis performed, is obvious that the UV/H2O2 advanced oxidation process has significant potential for removal of the phosphate esters, if the UV intensity in the reactor is increased. Further increase in the efficiency of the AOP process can be made by adding higher hydrogen peroxide doses (order of 1 to 5 mM). Such a design scheme is clearly focused in the advanced oxidation process rather than disinfection. The higher hydrogen peroxide doses will allow lower UV intensities in the reactor for the same removal but will require additional treatment stages for the removal of hydrogen peroxide from water. In any case, based on the required removal efficiency for the reactor the exact choices of the UV lamps power and the initial hydrogen peroxide dose are optimization issues.

The results of this work suggest that the UV/H_2O_2 process is very promising as an oxidation process but the economic cost prohibits large scale applications, for example DWTPs. What seems to be an economically feasible application for the UV/H_2O_2 process are industrial effluents. Since industrial effluents are highly regulated, the increased cost of the treatment process might be financially justifiable.

Even though UV/H2O2 advanced oxidation process is the most researched AOP, various issues require further study.

The mechanisms of hydroxyl radical reactions in aqueous solutions are not currently understood as clearly as the ones in the gas phase. Research towards developing structure-reactivity models for the aqueous phase is necessary because due to the immense number of environmental organic pollutants it is not possible to experimentally derive all of the reaction rate constants. In addition it would be very helpful if a model to predicting the possible intermediary products of the oxidation of various organic compounds from hydroxyl radical were developed.

In the model developed here, since the products of the oxidation of the phosphate esters are not known, their fate is not considered. One simplifying approach is to assume that the phosphate esters are completely mineralized to carbon dioxide and phosphoric acid. We feel that such an approach is oversimplifying and could yield worse results than just ignoring the products. Stefan, Hoy and Bolton (1996) present a kinetic model for the degradation of acetone in an UV/H2O2 process where the products are known. Their analysis is excellent and the results from their kinetic model agree very well with the observed experimental data. Therefore, we suggest that when designing such a treatment process targeting at specified organic chemicals, detailed experiments should be performed to establish the reaction mechanism concerning the products.

The model developed for this thesis considers the various other radicals emerging in the solution ($HO_2\bullet/O_2\bullet^-, CO_3^{2-}\bullet$) as non-reactive. This assumption was also made by Stefan, Hoy and Bolton (1996), Glaze, Lay and Kang (1995) and Crittenden et al. (1999). Even though these radicals are not expected to be as reactive as hydroxyl radical, it is clear that they react with organic chemicals to some extent. Therefore research must be done to at least identify the general pattern of their reactions and to establish some relevant reaction rates.

Finally, the chain reaction mechanism needs further investigation. The fate of the $HO_2\bullet/O_2\bullet^-$ radicals that are produced is probably dependent on the concentration of metal catalysts such as Fe and Cu in the solution. The possibility of a chain reaction mechanism significantly complicates the prediction of reaction rates but also suggests

that under certain conditions the reaction can be accelerated and the oxidation efficiency of the process greatly enhanced.

All of the issues stated above are well beyond the scope of this work. Because advanced oxidation processes are expected to find significant applications in the near future, research in the previous issues will prove very valuable for the environmental engineering science.

7 Bibliography

Buxton G.V., Greenstock C.L., Helman P.W., Ross A.B. (1988). Critical Review of Rate Constants for Reaction of Hydrated Electrons, Hydrogen Atoms and Hydroxyl Radicals ($^{\cdot}OH / ^{\cdot}O^{-}$) in Aqueous Solution. *J. Phys. Chem. Ref. Data* 17, 513-886

Crittenden J.C., Hu S., Hand D.W., Green S.A. (1999). A Kinetic Model for H2O2/UV Process in a Completely Mixed Batch Reactor, *Wat. Res. 33*

E.P.A. "Design Manual: Municipal Wastewater Disinfection", EPA/6251-86/021, 1986

Environmental Health Criteria, http://www.inchem.org/pages/ehc.html, February, 8, 2004

Glaze W.H, Lay Y.Kang J.W. (1995). Advanced Oxidation Processes. A Kinetic Model for the Oxidation of 1,2-Dibromo-3-chloropropane in Water by the Combination of Hydrogen Peroxide and UV Radiation, *Ind. Eng. Chem. Res. 34*

Haag W.R, Yao D.C.C. (1992). Rate Constants for Reaction of Hydroxyl Radicals with several drinking water Contaminants, *Env. Sci. Tech. 26*

HSDB database, part of TOXNET maintained by National Library of Medicine (NLM) http://toxnet.nlm.nih.gov/ (11/13/2003).

Kolpin D.W., Furlong E.T., Meyer M.T., Thurman M.E, Zaugg S.D., Barber L.B., Buxton H.T. (2002). Pharmaceuticals, Hormones, and Other Organic Wastewater Contaminants in U.S. Streams, 1999-2000:A National Reconnaissance. *Env. Sci. Tech. 36*

Lin, Joseph C. "Determining the Removal Effectiveness of Flame Retardants from Drinking Water Treatment Processes". Master of Engineering Thesis Massachusetts Institute of Technology, 2004.

Masschelein W.J. (2002). *Ultra Violet light in Water and Wastewater Sanitation*. Lewis Publishers

Notre Dame Radiation Laboratory, Radiation Chemistry Data Center, http://www.rad.nd.edu/rcdc/ (11/20/2004)

Schwarzenbach, R. P., Gschwend, P. M., Imboden, D. M.. (2003). *Environmental Organic Chemistry*, 2nd edition, Wiley-Interscience, New York

Stefan M.I, Hoy A.R, Bolton J.R. (1996). Kinetics and Mechanism of the Degradation and Mineralization of Aceton in Dilute Aqueous Solution Sensitized by the UV Photolysis of Hydrogen Peroxide, *Env. Sci. Tech. 30*

Stumm W., Morgan J.J. (1996). *Aquatic Chemistry*, 3rd edition, Wiley-Interscience, New York

Syracuse Research Corporation (SRC). Compiles physical properties of thousands of chemicals, located in the PHYSPROP database. Database last used on 12/4/2003.

APPENDIX: COMPUTER CODES

% AOP1- first essay

```
pH=6.6; % define constant pH
CTo=1*10^(-4);
TOTH2O2o=5*10^-4;    %define TOT H2O2 M
InitialH2O2=TOTH2O2o*(1+10^-11.6*10^pH)^-1; %calculate steady equilibtium conc
for H2O2
InitialHO2=TOTH2O2o-InitialH2O2; % HO2 t=0
InitialHCO3=CTo*(1+10^(pH-10.33)+10^(6.35-pH))^-1;
InitialH2CO3=10^(-pH+6.35)*InitialHCO3;
InitialCO3=10^(pH-10.33)*InitialHCO3;
InitialTBP=7*10^-11;
InitialTBEP=1.6*10^-9;
InitialTCEP=4*10^-10;
tspan=[0
20];species0=[TOTH2O2o;InitialH2O2;InitialHO2;0;0;0;0;CTo;InitialH2CO3;InitialHC
O3;InitialCO3;0;InitialTBP;InitialTBEP;InitialTCEP];    %assign initial values to
tspan,comp0
options=odeset('reltol',1e-6,'abstol',1e-20,'stats','on');
[t,species]=ode15s('FINAL',tspan,species0,options); % run ode23s
TOTH2O2=species(:,1);COHrad=species(:,4);CTOTHO2rad=species(:,5);CCO3rad=spe
cies(:,12);CHCO3=species(:,10);
CCO3=species(:,11);CTBP=species(:,13);CTBEP=species(:,14);CTCEP=species(:,15);C
H2O2=species(:,2);CHO2=species(:,3);CHO2rad=species(:,6);CO2rad=species(:,7);
%plot(t,CTBP,'b.',t,CTBEP,'bx',t,CTCEP,'b^')%,t,CTOTHO2rad,'y',t,CHO2rad,'o',t,CO2r
ad,'y.')   %plot compounds vs time
semilogy(t,COHrad,'r.',t,CTBEP,t,CTBP,t,CTCEP)%,t,CTOTHO2rad,'y',t,CHO2rad,'o',t,
CO2rad,'y.')   %plot compounds vs time
xlabel('t sec')
axis([0 20 10^-13 10^-3])
legend('[TBEP]','[TBP]','[TCEP]')
%legend('[OHrad]','[HCO3-]','[CO3]','[CO3rad]')
%title('Ct=10^-3   pH=8   Io=5*10^-3')
```

```
function speciesdt=final(t,species)
pH=6.6;
k2=2.7*10^7;
k3=7.5*10^9;
k4=3;
k5=0.13;
k6=3.9*10^8;
k7=8.5*10^6;
k8=4.3*10^5;
k9=3*10^7;
k10=5.5*10^9;
k11=6.6*10^9;
k12=8.3*10^5;
k13=9.7*10^7;
k14=7*10^9;
k15=3*10^9;
k16=6*10^8;
k17=3*10^7;
kTBP=10^10;
kTBEP=2*10^10;
kTCEP=2*10^9;
TOTH2O2=species(1);
H2O2=species(2);
HO2=species(3);
OHrad=species(4);
TOTHO2rad=species(5);
HO2rad=species(6);
O2rad=species(7);
CT=species(8);
H2CO3=species(9);
HCO3=species(10);
CO3=species(11);
CO3rad=species(12);
TBP=species(13);
TBEP=species(14);
TCEP=species(15);
Ab=(17.9*H2O2+228*HO2+0.02);
PHOTrate=-0.0222*Ab^6+0.03028*Ab^5-0.01657*Ab^4+0.004652*Ab^3-
0.0007102*Ab^2+5.639*10^(-5)*Ab-8.097*10^(-7);
%PHOTrate=5*(-0.0222*Ab^6+0.03028*Ab^5-0.01657*Ab^4+0.004652*Ab^3-
0.0007102*Ab^2+5.639*10^(-5)*Ab-8.097*10^(-7)); %5*
%PHOTrate=10*(-0.0222*Ab^6+0.03028*Ab^5-0.01657*Ab^4+0.004652*Ab^3-
0.0007102*Ab^2+5.639*10^(-5)*Ab-8.097*10^(-7));
%PHOTrate=100*(-0.0222*Ab^6+0.03028*Ab^5-0.01657*Ab^4+0.004652*Ab^3-
0.0007102*Ab^2+5.639*10^(-5)*Ab-8.097*10^(-7));
```

```
RTOTH2O2=-PHOTrate*H2O2-k2*H2O2*OHrad-k3*HO2*OHrad-k4*H2O2*HO2rad-
k5*H2O2*O2rad-k8*H2O2*CO3rad-
k9*HO2*CO3rad+k10*OHrad^2+k12*HO2rad^2+k13*HO2rad*O2rad;
ROHrad=2*PHOTrate*H2O2-k2*H2O2*OHrad-
k3*HO2*OHrad+k4*H2O2*HO2rad+k5*H2O2*O2rad-k6*OHrad*CO3-
k7*OHrad*HCO3-k10*OHrad^2-k11*OHrad*HO2rad-k14*OHrad*O2rad-
k15*OHrad*CO3rad-kTBP*OHrad*TBP-kTBEP*OHrad*TBEP-kTCEP*OHrad*TCEP;
RTOTHO2rad=k2*H2O2*OHrad+k3*HO2*OHrad-k4*HO2rad*H2O2-
k5*O2rad*H2O2+k8*H2O2*CO3rad+k9*CO3rad*HO2-k11*HO2rad*OHrad-
k12*HO2rad^2-k13*HO2rad*O2rad-k14*O2rad*OHrad-k16*O2rad*CO3rad;
RCO3rad=k6*OHrad*CO3+k7*OHrad*HCO3-k8*CO3rad*H2O2-k9*CO3rad*HO2-
k15*CO3rad*OHrad-k16*CO3rad*O2rad-k17*CO3rad^2;
RCT=-k7*HCO3*OHrad+k8*CO3rad*H2O2-
k6*CO3*OHrad+k9*CO3rad*HO2+k16*CO3rad*O2rad;
RTBP=-kTBP*OHrad*TBP;
RTBEP=-kTBEP*OHrad*TBEP;
RTCEP=-kTCEP*OHrad*TCEP;
RH2O2=RTOTH2O2/(1+10^(-11.6+pH));
RHO2=RTOTH2O2/(1+10^(11.6-pH));
RHO2rad=RTOTHO2rad*(1+10^(pH-4.8))^-1;
RO2rad=RTOTHO2rad/(1+10^(4.8-pH));
RHCO3=RCT*(1+10^(6.35-pH)+10^(pH-10.33))^(-1);
RH2CO3=RCT*(1+10^(pH-6.35)+10^(2*pH-16.68))^(-1);
RCO3=RCT*(1+10^(10.33-pH)+10^(16.68-2*pH))^(-1);
speciesdt=[RTOTH2O2;RH2O2;RHO2;ROHrad;RTOTHO2rad;RHO2rad;RO2rad;RCT;
RH2CO3;RHCO3;RCO3;RCO3rad;RTBP;RTBEP;RTCEP];
```

```
%Min_intensity
A=0.04;
Izn=0;
Izo=0;
Iline=0;
Io=0;
r=50;

for m=1:200
zo=m;
   for n=1:200
   zn=abs(zo-n);
   Izn=(1/(200*4*3.14*(r^2+zn^2)))*exp(-A*(r^2+zn^2)^(0.5));
   Izo=Izo+Izn;
   end
   Iline=Iline+Izo;
   Izo=0;
end

Io=0.04/(20*Iline/200);
```

```
%phot_abs
Io=9.77*10^-4;
H2O2=0;
Awat=0.02;

Izn=0;
Izo=0;
P1deg=0;
P1dvol=0;
Pav=0;

OutMatrix=[];
Outline=[];
plot_matrix=[];

In=[];  %create intensity matrix
Arean=[];   ;%create area matrix
Area=0;
Pcross=[];  %create absorbed photons per cross section matrix

%calculate the area matrix
   for r=1:49
      Area=3.14159*(r+1+r)/360;
      Arean=[Arean; Area];
   end



%calculate for various absorbances
for H2O2=0.0001:0.001:0.02

Pav=0;

A=17.9*H2O2+0.02;

Pcross=[];


for l=1:200

    %clear intensity matrix
   In=[];

   zo=l;

   Izo=0;
```

```
  %calculate the intensity matrix for cross section
  for r=1:50
     for n=1:200
     zn=abs(zo-n);
     Izn=(Io/(200*4*3.14*(r^2+zn^2)))*exp(-A*(r^2+zn^2)^(0.5));
     Izo=Izo+Izn;
     end

     In=[In; Izo];
     Izo=0;  %to clear the previous number
  end

  %calculate absorbed photons per degree (not in 2.3eH2O2)
  for r=1:49
     P1deg=P1deg+((In(r+1)+In(r))/2)*Arean(r);   %units (ein)
  end

  %calculate absorbed photons per 1 deg volume and account for 2.3*H2O2*e
  P1dvol=2.3*H2O2*17.9*P1deg/(3.14*50^2-3.14*1^2);  %units (ein/cm3)

  %calculate absorbed photons per volume per cross section
  Pcross=[Pcross; P1dvol*360];

  %make P1deg value zero for next loop
  P1deg=0;

end

  %find average absorbed photons per cross section
  for i=1:200
     Pav=Pav+Pcross(i);
  end
  Pav=Pav/200;
  %create output matrix
  Outline=[H2O2 A Pav];

  %create Output matrix
  OutMatrix=[OutMatrix; Outline];

  %create matrix for plots
  plot_matrix=[plot_matrix; H2O2 A 1000*Pav 1000*Pav/H2O2];
  %clear Outline
  Outline=[];

    end
```